Chemical and electrochemical water oxidation mediated by bis(pyrazol-1-ylmethyl)pyridine-ligated Cu(I) complexes

T Makhado,[a] B Das,[b] RJ Kriek,[c] HCM Vosloo[a] and AJ Swarts[a]*

[a] Catalysis and Synthesis Research Group, Research Focus Area: Chemical Resource Beneficiation, North-West University, 11 Hoffman Street, Potchefstroom 2531, South Africa

[b] Department of Organic Chemistry, Arrhenius Laboratory Stockholm University, Svante Arrhenius väg 16C, 10691 Stockholm, Sweden

[c] Electrochemistry for Energy & Environment Group, Research Focus Area: Chemical Resource Beneficiation, North-West University, 11 Hoffman Street, Potchefstroom 2531, South Africa

Supplementary Information

Experimental Section

General considerations

Reagents for the synthesis of ligands such as 3,5-dimethylpyrazole, 2,6-bis(chloromethyl)pyridine, 2-(chloromethyl)-pyridine hydrochloride, hydrazine monohydrate were purchased from Sigma Aldrich and used as received. The pyrazolyl ligand precursors, 3,5-di-tert-butyl-1H-pyrazole and 3,5-diphenyl-1H-pyrazole, were synthesized following literature procedures.[1] (Pyrazol-1-ylmethyl)pyridine ligands were synthesized following literature procedures.[2] All moisture and oxygen-sensitive reactions were performed using Schlenk techniques. The solvents were distilled under a nitrogen atmosphere using Na metal for diethyl ether and CaH_2 for dichloromethane as drying agents. NMR (^1H and ^{13}C) spectra were recorded on a Bruker Ultrashield Plus at 600 MHz and 151 MHz respectively. FTIR analysis were done on a BruckerAlpha-P range infrared instrument equipped with ATR in the range of 400 cm^{-1} to 4000cm^{-1}. Magnetic susceptibility studies were done using a Sherwood Scientific MK1 with 4mm diameter sample tubes containing 50 mM of the sample. Mass spectrometry was performed on BrickermicroTOF-Q II mass spectrometer. Elemental analysis was performed on a Perkin Elmer 2400 Elemental Analyzer. Cyclic voltammetry studies were done on a BioLogic VSP potentiostat employing a water-jacketed electrochemical cell connected to a refrigerated temperature controller (Julabo F-12 ED). DLS analysis were performed on a Mastersizer 2000 Ver. 5.60 from Malvern instruments.

Section S1: Synthesis of Ligands and complexes and crystallographic data collection:

Synthesis of 2,6-bis((3,5-dimethyl-1H-pyrazol-1-yl)methyl)pyridine (MePzPy) (L2)

Following the same synthetic procedure as **L1**, **L2** was synthesised from 2,6-bis(chloromethyl)pyridine (0.5 g, 2.84 mmol) and 3,5-dimethyl-1H-pyrazole (0.55g, 5.68 mmol). The product was isolated as a white solid. Yield: 0.79 g (95 %).^1H NMR: (600 MHz, ppm, CD_2Cl_2): δ 2.18 (s, 12H,C**H**$_3$ (*pz*)), 5.25 (s, 4H, C**H**$_2$), 5.85 (s, 2H,4-**H** (*pz*)), 6.69 (d, 2H, **H**$_\beta$ (*py*), $^2J_{HH}$ = 12.0 Hz) 7.54 (t, 1H, **H**$_\gamma$ (*py*), $^3J_{HH}$ = 12 Hz).^{13}**C**{^{1}H} NMR: (150 MHz, ppm, $CDCl_3$): δ 11.39 (5-**C**H$_3$), 1C39 (3-**C**H$_3$), 54.74 (**C**H$_2$), 105.84 (4-**C** (*pz*)), 120.19 (**C**$_\beta$ (*py*)) 138.38(**C**$_\gamma$ (*py*)),140.25 (3-**C** (*pz*)), 148.05 (5-**C** (*pz*)) 157.82 (**C**$_q$). FTIR (ATR) *v* cm^{-1}: 1579 (C=N) (py).

Synthesis of 2,6-bis((3,5-di-tert-butyl-1H-pyrazol-1-yl)methyl)pyridine (*t*-BuPzPy) (L3)

L3 was synthesized from 2,6-bis(chloromethyl)pyridine (0.25 g, 1.42 mmol) and 3,5-di-tert-butyl-1H-pyrazole (0.51g, 2.84 mmol) in the same manner as the synthesis of **L1**. The product was isolated as a pale-yellow solid. Yield: 0.304 g (46 %).^1H NMR: (600 MHz, ppm, $CDCl_3$): δ 1.24 (s, 18H, 5-(C**H**$_3$)$_3$ (*pz*)), 1.30 (s, 18H, (3-C**H**$_3$)$_3$ (*pz*)), 5.53 (s, 4H, C**H**$_2$), 5.91 (s, 2H,4-**H** (*pz*)), 6.28 (d, 2H, **H**$_\beta$ (*py*), $^2J_{HH}$ = 6.0 Hz) 7.39 (t, 1H, **H**$_\gamma$ (*py*), $^3J_{HH}$ = 6.0 Hz). ^{13}**C**{^{1}H} NMR: (150 MHz, ppm, $CDCl_3$): δ 30.2 (5-(**C**H$_3$)$_3$), 30.6(3-(**C**H$_3$)$_3$), 31.32 (5-**C**(CH$_3$)$_3$), 31.95 (3-**C**(CH$_3$)$_3$), 56.31(**C**H$_2$), 100.54 (4-**C** (*pz*)), 118.93 (**C**$_\beta$ (*py*)) 137.82 (**C**$_\gamma$ (*py*)), 152.04 (5-**C** (*pz*)), 157.02 (**C**$_q$), 160.77 (3-**C** (*pz*)).FTIR (ATR) *v* cm^{-1}: 1593 (C=N) (py).

Synthesis of 2,6-bis((3,5-diphenyl-1H-pyrazol-1-yl)methyl)pyridine (PhPzPy) (L4)

L4 was prepared from 2,6-bis(chloromethyl)pyridine (0.5 g, 2.84 mmol) and 3,5-diphenyl-1H-pyrazole (1.25 g, 5.68 mmol) following the same procedure as the synthesis of **L1**. The product was isolated as a white solid. Yield: 1.44 g (93 %) ^{1}**H** NMR: (600 MHz, ppm, $CDCl_3$): δ 5.45 (s, 4H, C**H**$_2$), 6.67 (s, 2H, 4-**H** (*pz*)), 6.87(d, 2H, **H**$_\gamma$, $^{2}J_{HH}$= 6 Hz), 7.30-7.35 (m,16H, Ph) 7.47 (t,1H, **H**$_\gamma$, $^{3}J_{HH}$ = 6.0 Hz) 7.84 (d, 4H, Ph, J_{HH} = 12 Hz). ^{13}**C**{^{1}H} NMR: (150 MHz, ppm, $CDCl_3$): δ 54.74 (**C**H_2), 10C26(4-**C** (*pz*)), 119.91 (**C**$_\beta$ (*py*)) 137.99(**C**$_\gamma$ (*py*)),139.75 (3-**C** (*pz*)), 148.05 (5-**C** (*pz*)) 157.02 (**C**$_q$). FTIR (ATR) *v* cm^{-1}: 1575 (C=N) (py).

Synthesis of [Cu

Synthesis of [Cu(I)(MePzPy)]PF_6 (C2)

A solution of 2,6-bis((3,5-dimethyl-1H-pyrazol-1-yl)methyl)pyridine (**L2**, 0.074 g, 0.25 mmol) in 2.5 mL dichloromethane was added to a solution of tetrakis(acetonitrile)copper(I) hexafluorophosphate ($Cu(MeCN)_4PF_6$) (0.094 g, 0.25 mmol) in 2.5 mL dichloromethane. The resulting yellow solution was stirred under argon for 2 hours. The addition of diethyl ether resulted in the precipitation of the complex. The complex was isolated as a yellow solid. Yield: 0.0910 g (72 %). ^{1}H NMR (**C2**): (600 MHz, ppm, CD_2Cl_2): δ 2.43 (s, 6H, 5-C**H**$_3$ (*pz*)), 2.45 (s, 6H, 3-C**H**$_3$ (*pz*)), 5.21 (s, 4H, C**H**$_2$), 6.10 (s, 2H,4-**H** (*pz*)), 7.61 (d, 2H, **H**$_\beta$ (*py*), $^{2}J_{HH}$ = 6.0 Hz) 8.01 (t, 1H, **H**$_\gamma$ (*py*), $^{3}J_{HH}$ = 6.0 Hz).^{13}**C**{^{1}H} NMR: (150 MHz, ppm, $CDCl_3$): δ 12.07 (5-**C**H_3), 15.31 (3-**C**H_3), 51.57 (**C**H_2), 106.89 (4-**C** (*pz*)), 124.59 (**C**$_\beta$ (*py*)) 138.38(**C**$_\gamma$ (*py*)),141.52 (3-**C** (*pz*)), 147.40 (5-**C** (*pz*)) 152.90 (**C**$_q$). ESI-MS (m/z): 358.11 $[M]^+$. FTIR (ATR) v cm^{-1}: 1600 (C=N). Analysis calc. (found) for $C_{17}H_{21}CuF_6N_5P$: C 40.52 (40.16); H 4.20 (3.93); N 13.90 (13.24).

Synthesis of [Cu(I)(*t*-BuPzPy)]PF_6 (C3)

A solution of 2,6-bis((3,5-di-tert-butyl-1H-pyrazol-1-yl)methyl)pyridine (**L3**, 0.116 g, 0.25 mmol) in 2.5 mL dichloromethane was added to a solution of tetrakis(acetonitrile)copper(I) hexafluorophosphate ($Cu(MeCN)_4PF_6$) (0.094 g, 0.25 mmol) in 2.5 mL dichloromethane. The resulting yellow solution was stirred under argon for 2 hours. The addition of diethyl ether resulted in the precipitation of the complex. The complex was isolated as a yellow solid. Yield: 0.1173 g (70%). ^{1}H NMR: (600 MHz, ppm, $CDCl_3$): δ 1.45 (s, 18H, 5-(C**H**$_3$)$_3$ (pz)), 1.54 (s, 18H, (3-C**H**$_3$)$_3$ (pz)), 5.53 (s, 4H, C**H**$_2$), 6.02 (s, 2H,4-**H** (pz)), 7.68 (d, 2H, **H**$_\beta$ (py), $^{2}J_{HH}$ = 6.0 Hz) 7.97 (t, 1H, **H**$_\gamma$ (py), $^{3}J_{HH}$ = 6.0 Hz).^{13}**C**{^{1}H} NMR: (150 MHz, ppm, $CDCl_3$): δ 30.19 (5-(**C**H_3)$_3$), 31.35 (3-(**C**H_3)$_3$), 31.75 (5-**C**$(CH_3)_3$), 32.27 (3-**C**$(CH_3)_3$), 5C15(**C**H_2), 101.97 (4-**C** (pz)), 124.14 (**C**$_\beta$ (py)) 141.05(**C**$_\gamma$ (py)), 151.55 (5-**C** (pz)), 154.91(**C**$_q$), 162.45 (3-**C** (pz)).ESI-MS (m/z): 526.30 $[M]^+$. FTIR (ATR) v cm^{-1}: 1604 (C=N). Analysis calc. (found) for $C_{29}H51CuF_6N_5O_3P$: C 47.96 (47.45); H 7.08 (6.05); N, 9.64 (8.69).

Synthesis of [Cu(I)(PhPzPy)]PF_6 (C4)

A solution of 2,6-(3,5-diphenyl-1H-pyrazol-1-yl)methyl)pyridine (**L4**, 0.136 g, 0.25 mmol) in 2.5 mL dichloromethane was added to a solution of tetrakis(acetonitrile)copper(I) hexafluorophosphate ($Cu(MeCN)_4PF_6$) (0.094 g, 0.25 mmol) in 2.5 mL dichloromethane. The resulting yellow solution was stirred under argon for 2 hours. The addition of diethyl ether resulted in the precipitation of the complex. The complex was isolated as a yellow solid. Yield: 0.1220 g (65 %)^{1}**H** NMR: (600 MHz, ppm, Acetone-

d_6): δ 5.71 (s, 4H, C**H**$_2$), 7.09 (s, 2H, 4-**H** (pz)), 7.35(d, 2H, **H**$_\gamma$, $^2J_{HH}$= 6 Hz), 7.63-7.68 (m,16H, Ph(**H**)) 7.97 (t,1H, **H**$_\gamma$, $^3J_{HH}$ = 6.0 Hz) 8.11 (d, 4H, Ph(**H**), J_{HH} = 12 Hz).^{13}**C**{^{1}H} NMR: (150 MHz, ppm, Acetone-d_6): δ 53.12 (**C**H$_2$), 128.42(4-**C** (pz)), 129.64 (**C**$_\beta$ (py)) 130.25(**C**$_\gamma$ (py)),130.39 (3-**C** (pz)), 131.12 (5-**C** (pz)) 132.39 (**C**$_q$) . ESI-MS (m/z): 606.17 $[M]^+$. FTIR (ATR) ν cm^{-1}: 1597 (C=N). Analysis calc. (found) for $C_{37}H_{31}CuF_6N_5OP$: C 57.70 (57.85); H 4.06 (C34); N, 9.09 (8.45).

Crystallographic data collection

Single crystals of **C2**, **C3,** and **C4** were mounted on a nylon loop and centred in a stream of liquid nitrogen at 293(2) K. Crystal evaluation and data collection were performed on a Bruker D8 Quest Eco diffractometer with Mo Kα radiation (λ = 0.71073 Å). Data collection, reduction, and refinement were performed using SAINT[3]and SADABS,[4] which form part of the APEX3 software package.[5] The structures were solved by direct methods and refined by full-matrix least-squares on F^2 using SHELX-2016[6] within the X-seed graphic user interface.[7] All non-hydrogen atoms were refined anisotropically and all hydrogen atoms were placed using calculated positions and riding models. Crystal structures of **C2**-**C4**, with accession numbers CCDC 2034903-2034905, available from the CCDC.

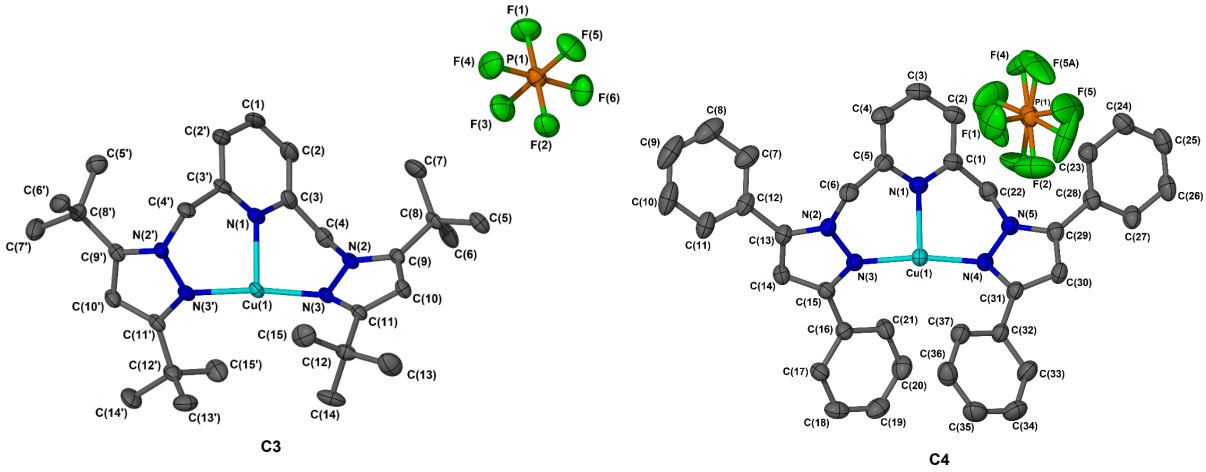

Figure S1: Ellipsoid diagrams of **C3** and **C4** respectively, drawn at 50% probability. Hydrogen atoms were omitted for clarity.

Table S1**:** Crystal data and refinement for **C2, C3,** and **C4**.

Parameter	**C2**	**C3**	**C4**
Chemical formula	$3.5_7H_{21}CuF_6N_5P$	$3.6_9H_{45}CuF_6N_5P$	$3.7_6H_{28}CuF_6N_6P$
Formula weight (g/mol)	503.90	670.21	753.15
Temperature (K)	293(2)	293(2)	273(2)
Wavelength (Å)	0.71076	0.71076	0.71076
Crystal size (mm)	0.200 x 0.200 x 0.200	0.200 x 0.200 x 0.200	0.097 x 0.111 x 0.279
Crystal system	Monoclinic	Orthorhombic	monoclinic
Space group	P 1 21/n 1	P 21 21 21	P 1 21/c 1
a (Å)	8.2344(6)	11.3842(9)	a = 11.7594(5)
b (Å)	14.8317(10)	15.6425(10)	23.6227(11)
c (Å)	17.2444(12)	18.2628(13)	13.1379(6)
α (deg) (̊)	90	90	90
β (deg)(̊)	95.076(5)	90	112.115(2)
γ (deg)(̊)	90	90	90
Volume ($Å^3$)	2097.8(3)	3252.2(4)	3381.1(3)
Z	4	4	4
D_{calc} (g/cm^3)	1.589	1.369	1.480
Absorption coefficient (mm^{-1})	1.182	0.781	0.763
F(000)	1020	1404	1536
Goodness of Fit on F^2	1.287	1.192	1.496
Final R_1 indices [I>2σ(I)]	0.0799	0.0507	0.664
wR_2 [I>2σ(I)]	0.1818	0.1369	0.1951

Table S2: Selected bond lengths and bond angles for **C2**, **C3,** and **C4**.

Bond lengths (Å)	**C2**	**C3**	**C4**
Cu1-N1	2.075(4)	2.110(3)	2.101(3)
Cu1-N3	2.077(5)	1.924(4)	1.910(2)
Cu1-N3′	2.058(5)	1.940(4)	1.907(2)
Bond Angles (Deg) ()			
N1-Cu1-N3′	89.2(2)	92.3(2)	95.41(1)
N1-Cu1-N3	97.6(2)	93.9(1)	93.41(1)
N3′-Cu1-N3	173.2(2)	173.2(2	171.12(1)

Table S3: The effect of a chemical oxidant on the TON and TOF of water oxidation.

Oxidant	**Concentration (mM)**	**[a]TON (mol O_2/mol Cu)**	**[b]TOF (mol O_2/mol Cu).s^{-1}**
CAN ($Ce(NH_4)_2(NO_3)_6$)	110	4.60	0.31
Sodium-*m*-periodate ($NaIO_4$)	110	3.77	0.14
Sodium persulfate ($Na_2S_2O_8$)	110	4.02	0.044

Reaction conditions: 25 µM, Solvent: MeCN:H_2O (1:1, 2 mL). **a** TON after 5 minutes reaction time. **b** TOF was calculated from the slope of the first 5 seconds on the TON curve.

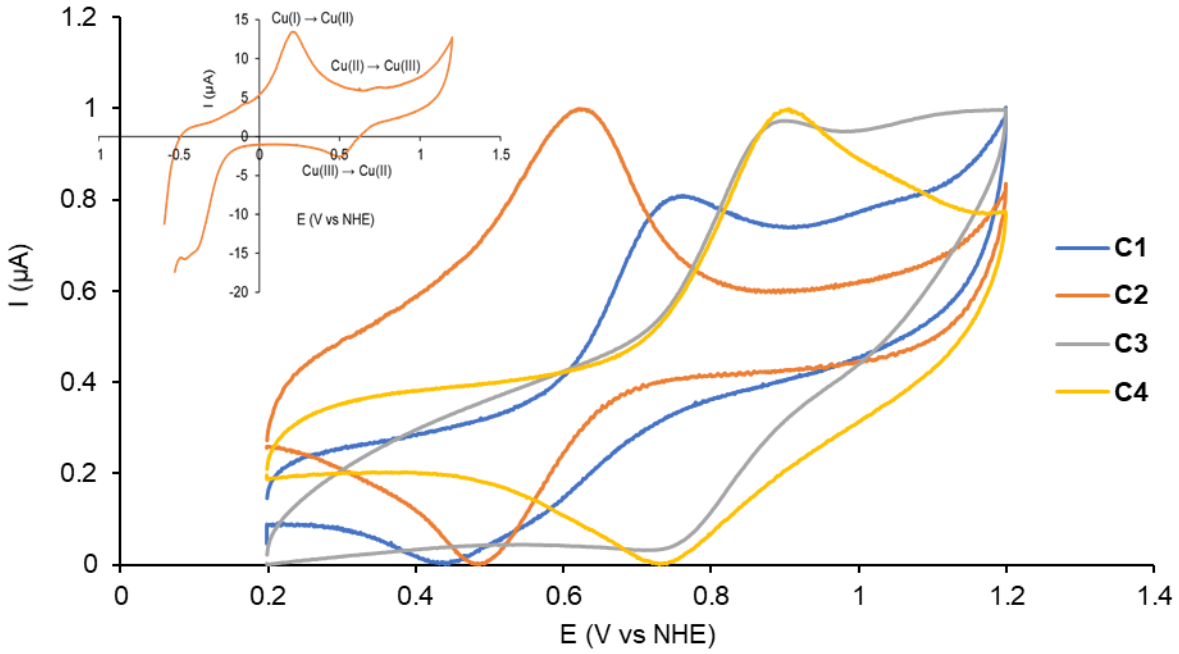

Figure S2: Cyclic voltammograms of the Cu(I) complexes (0.5 mM) performed in 0.1 M Bu_4NPF_6 in acetonitrile with the glassy carbon as the working electrode, platinum wire as counter electrode, and Ag/AgCl as the reference electrode. The scan rate was 10 mV s^{-1}. The reversible waves showing the reversible Cu(III)/Cu(II) couple of **C1-C4**. Inset: A CV showing irreversible wave assigned to the first oxidation of Cu(I) to Cu(II) for complex **C2**.

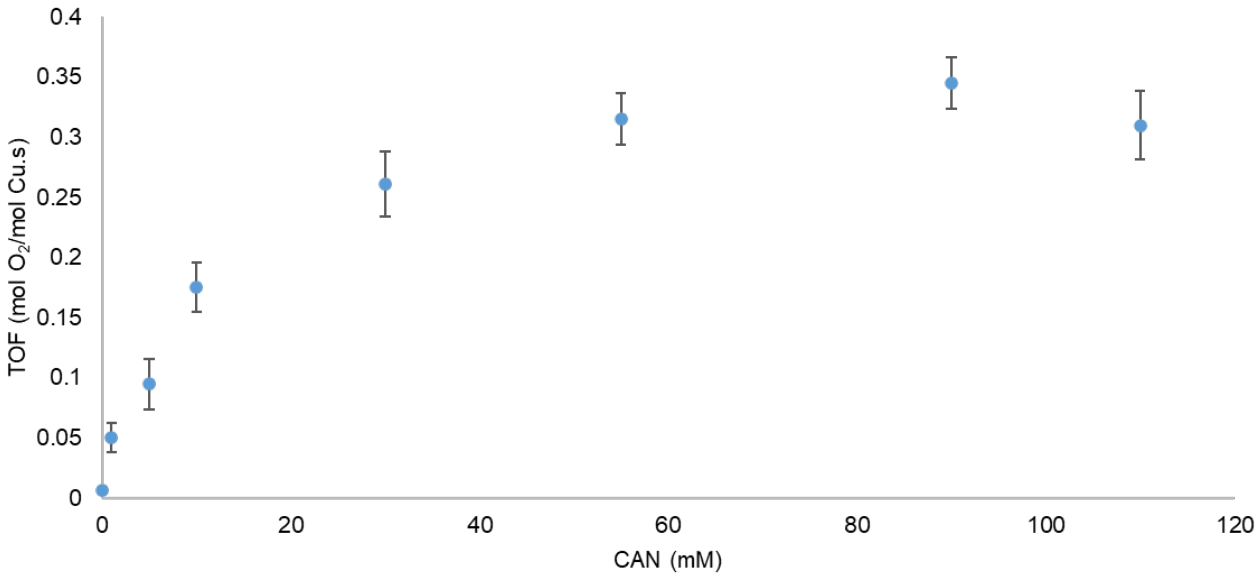

Figure S3: Effect of [CAN] on the activity of the catalyst studied using 25 µM **C2**.

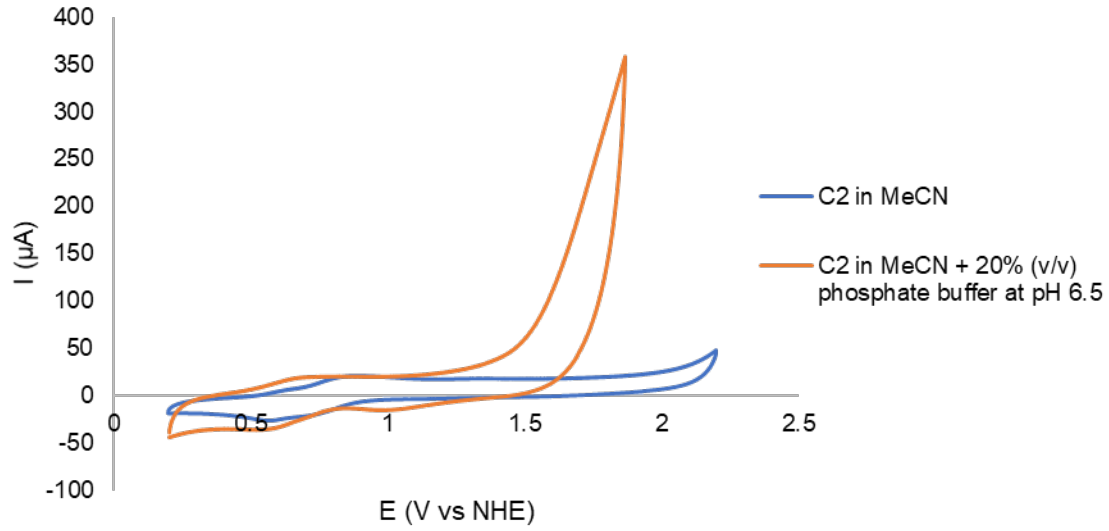

Figure S4: CVs of Cu(I) complex **C2** [0.5 mM] in a solution of MeCN and 0.1 M NBu_4PF_6 (Blue) and **C2** [0.42 mM] in a mixture of MeCN and 20% (v/v) phosphate buffer (0.2 M, pH 6.5) (Orange) recorded at a scan rate of 100 mV s^{-1}.

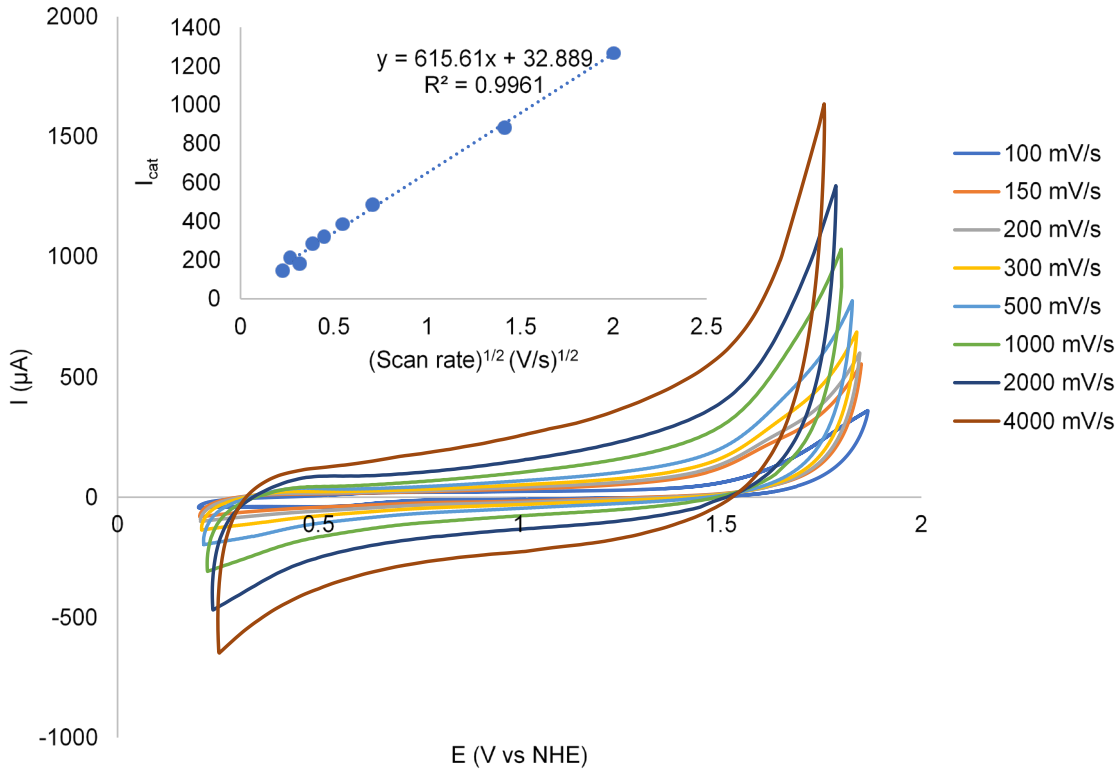

Figure S5: Scan rate dependence of 0.42mM **C2** scanned at 100-4000 mV/s. Inset: Linear scan rate dependence of the catalytic current at 1.7 V versus the square root of the scan rate.

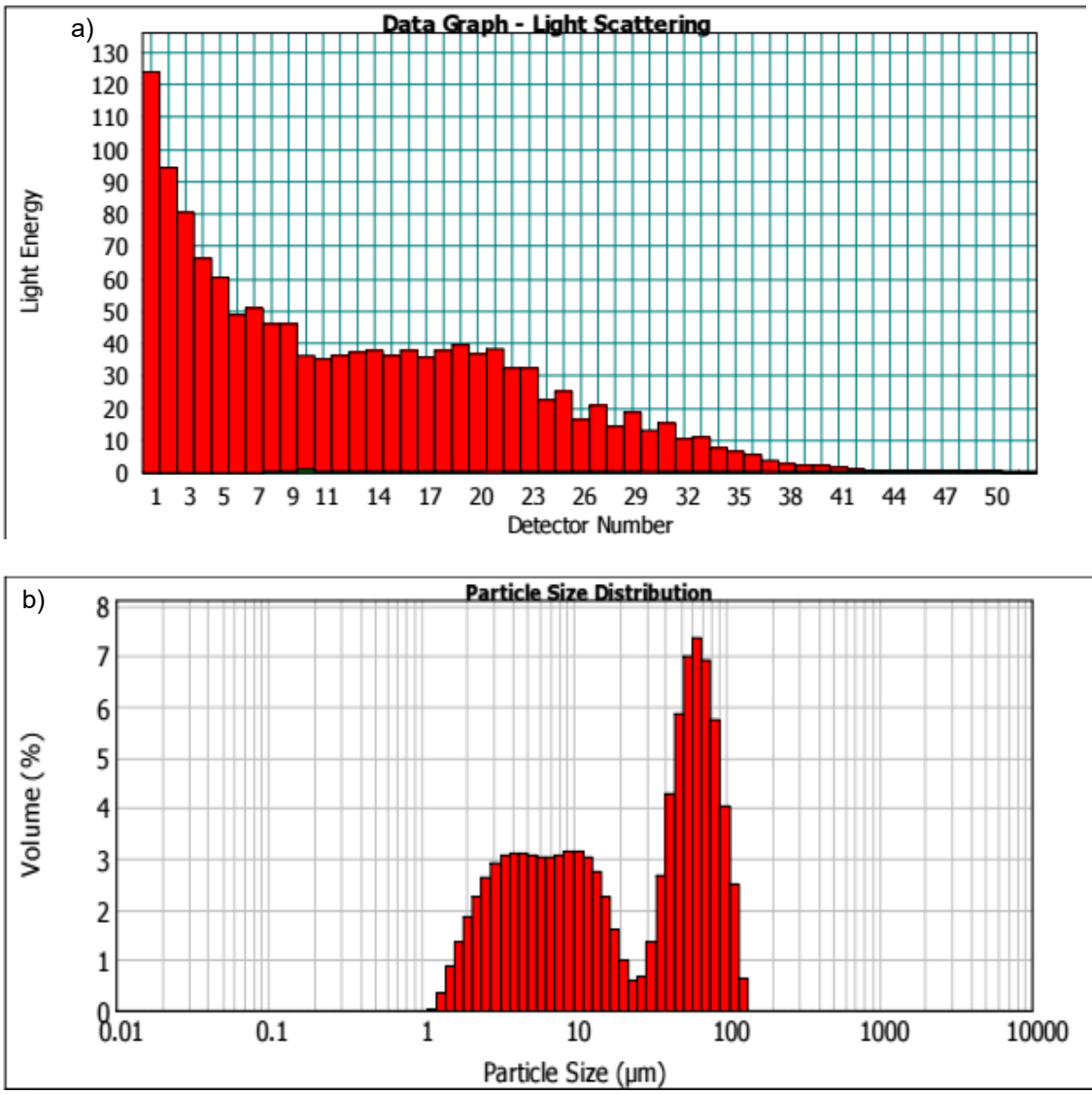

Figure S6: a) Data graph of the background against a 0.42 mM **C2** in a mixture of MeCN and 20% (v/v) phosphate buffer (0.2 M, pH 6.5) in the absence of the electrolyte. b) Particle distribution in the absence of the supporting electrolyte determined by DLS measurements post-electrolysis of 0.42 mM **C2** in a mixture of MeCN and 20% (v/v) phosphate buffer (0.2 M, pH 6.5).

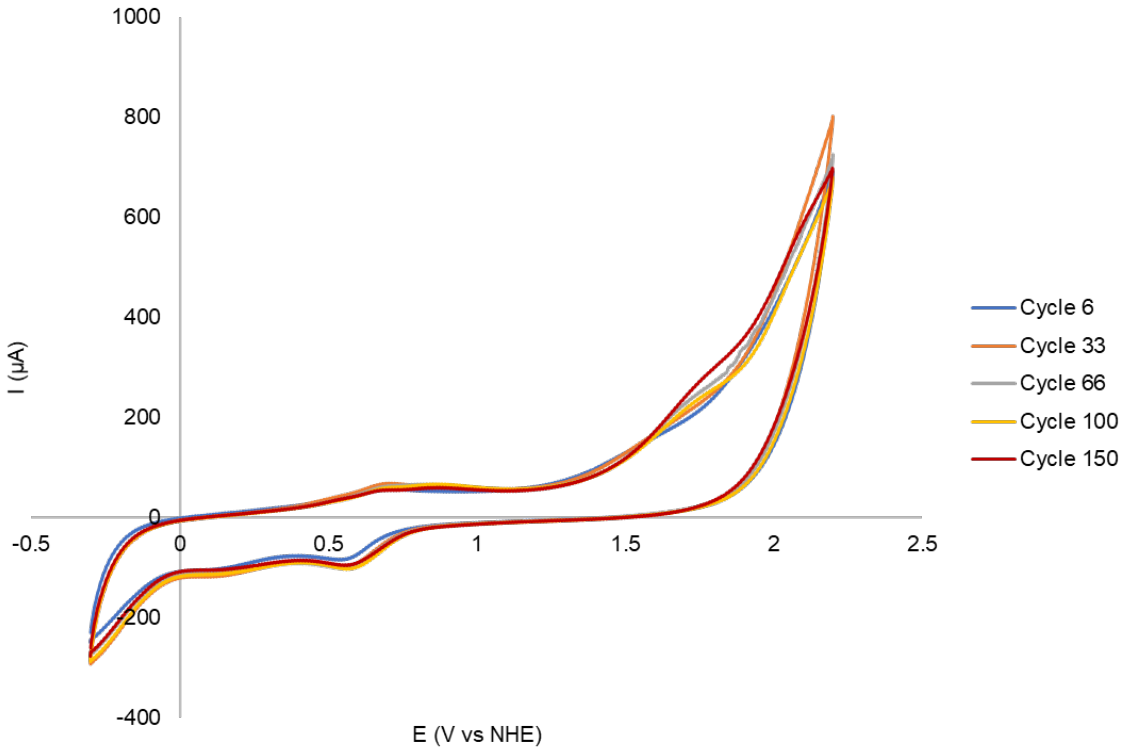

Figure S7: CVs in a mixture of MeCN and 20% (v/v) phosphate buffer (0.2 M, pH 6.5) of 0.42 mM **C2** scanned 150 times at a scan rate of 100 mV s^{-1}.

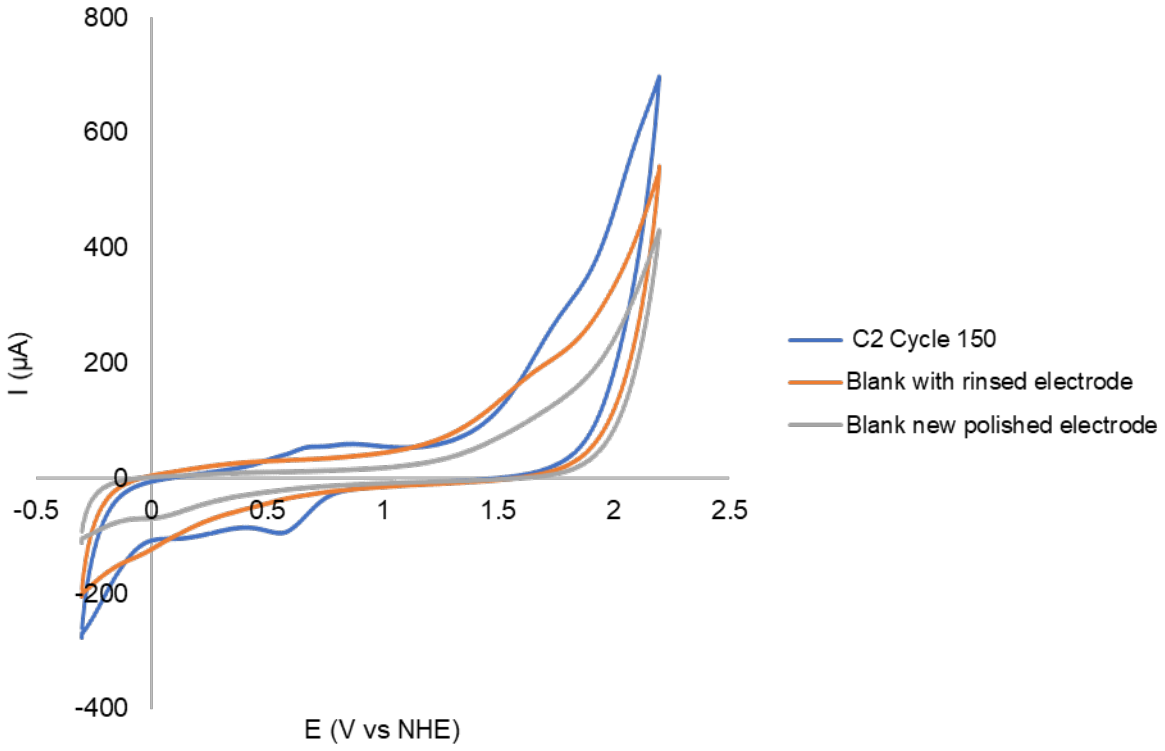

Figure S8: CVs in a mixture of MeCN and 20% (v/v) phosphate buffer (0.2 M, pH 6.5) of 0.42 mM **C2** (blue) after 150 cycles, followed by rinsed electrode in a fresh blank solution (orange) and a new polished electrode in blank solution (grey), recorded at a scan rate of 100 mV s^{-1}.

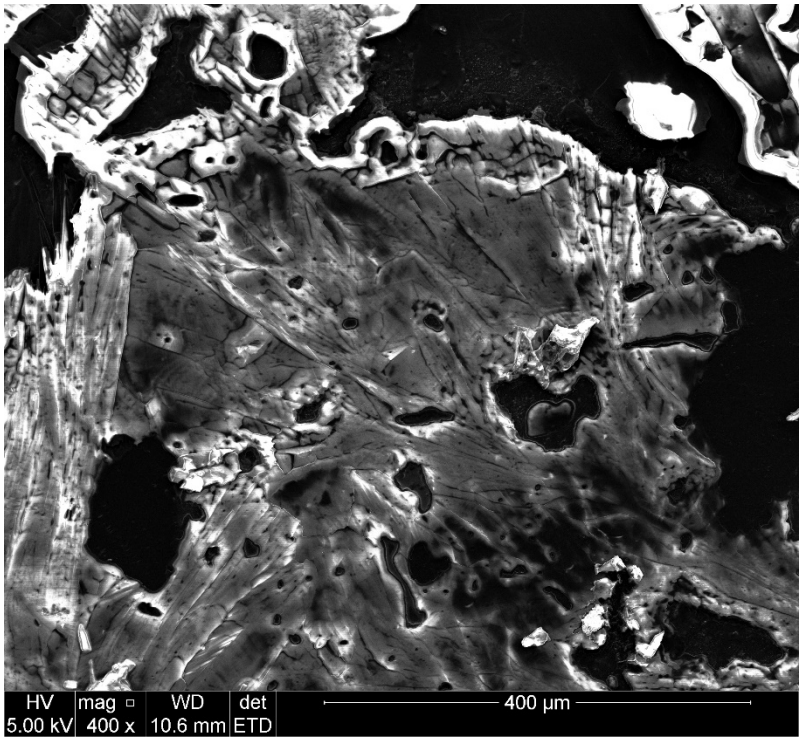

Figure S9: SEM image of the glassy carbon electrode post-electrolysis of a solution of **C2** in a mixture of MeCN, NBu_4PF_6 and 20% (v/v) 0.2 M phosphate buffer at pH 6.5 after 33 cycles.

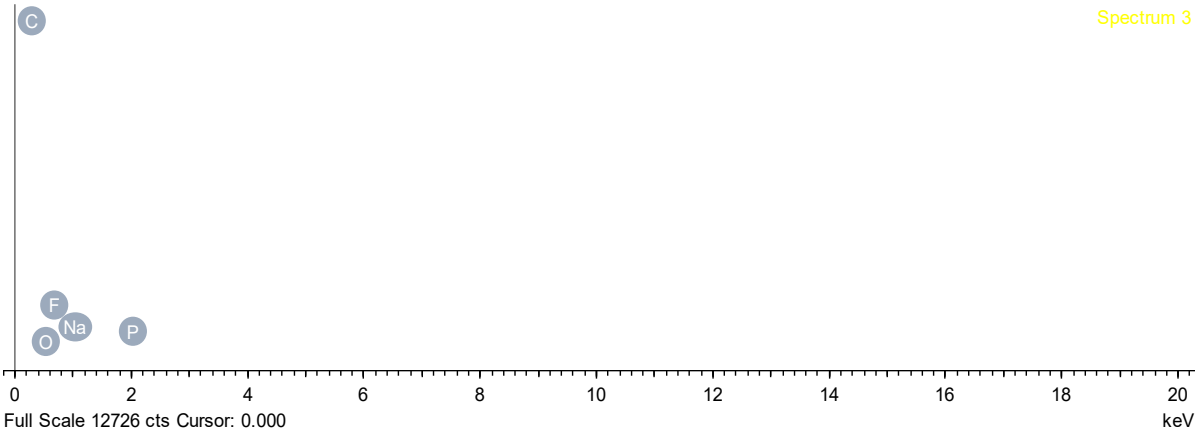

Figure S10: EDX pattern showing the absence of CuO nanomaterials on the glassy carbon electrode post electrolysis after 33 cycles.

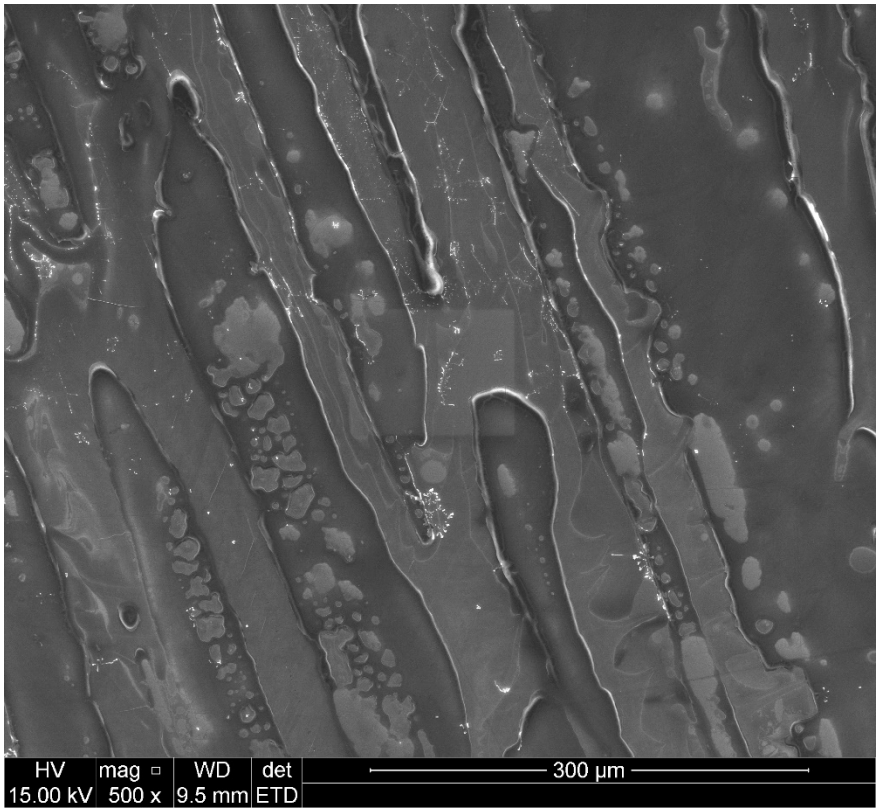

Figure S11: SEM image of the glassy carbon electrode post-electrolysis of a solution of **C2** in a mixture of MeCN, NBu_4PF_6 and 20% (v/v) 0.2 M phosphate buffer at pH 6.5 after 150 cycles.

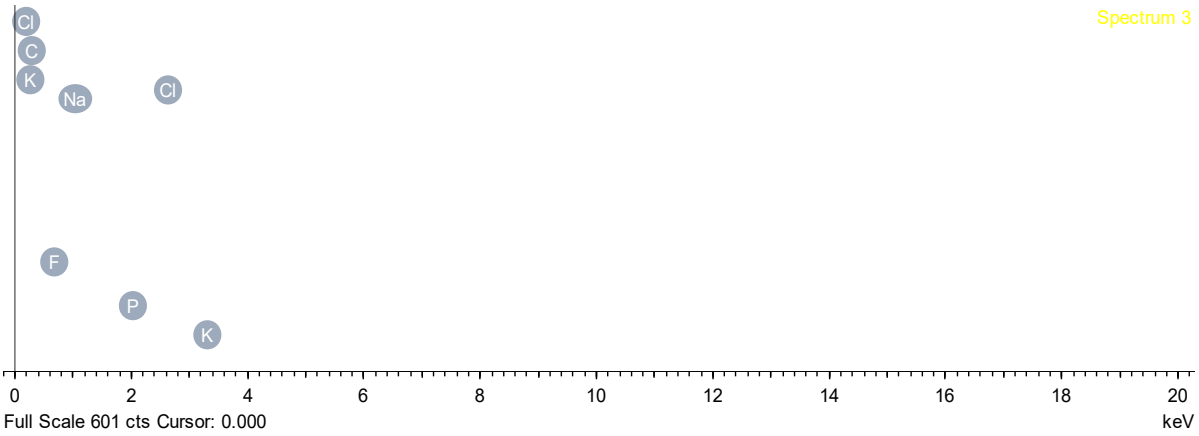

Figure S12: EDX pattern showing the absence of CuO nanomaterials on the glassy carbon electrode post electrolysis after 150 cycles. The potassium and the chloride ions are from the KCl solution which leached from Ag/AgCl reference electrode over time.

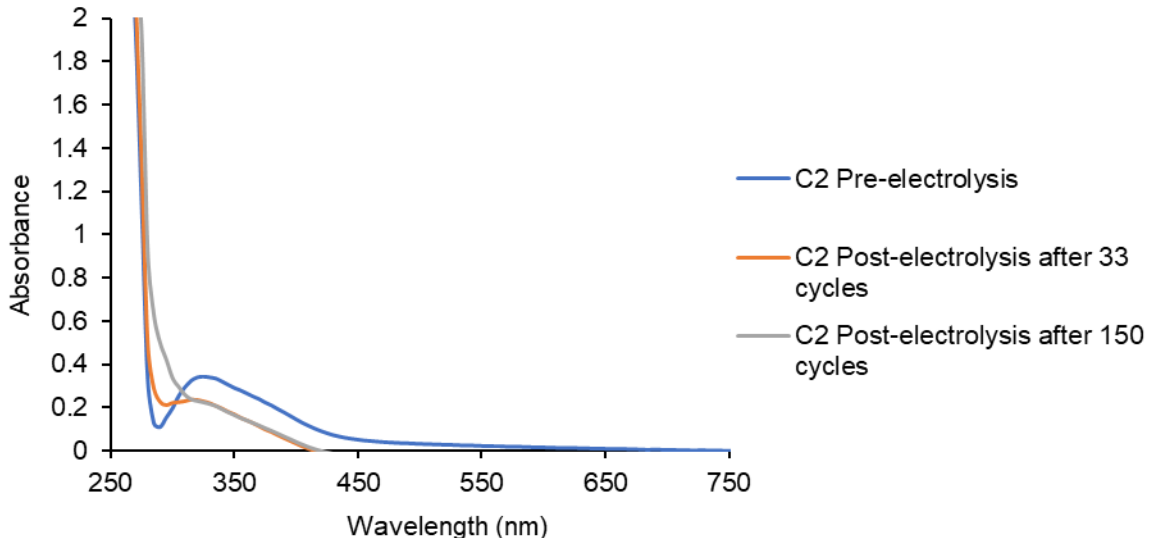

Figure S13: UV-Vis spectrums showing 0.42 mM **C2** in a in a solution of MeCN, NBu_4PF_6 and 20% (v/v) 0.2 M phosphate buffer at pH 6.5 before electrolysis (blue), post-electrolysis after 33 cycles (orange) and post electrolysis after 150 cycles (grey).

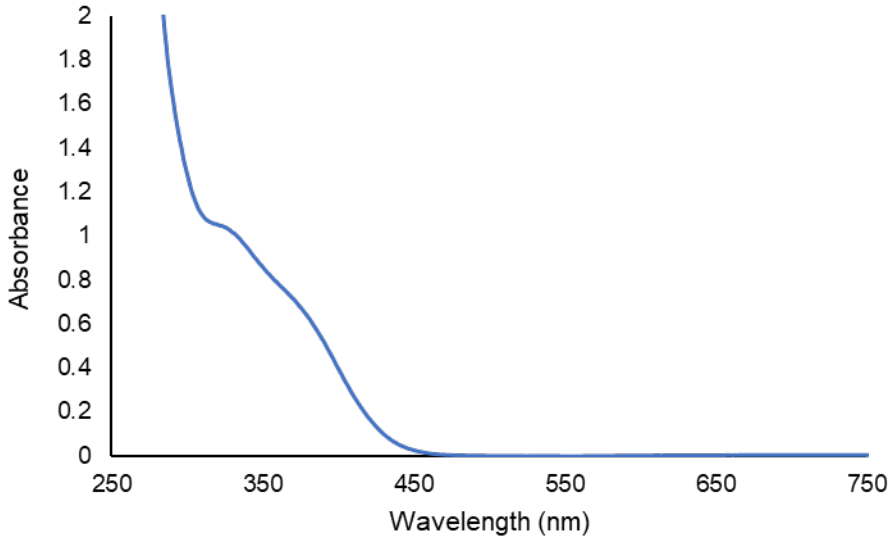

Figure S14: UV-Vis spectrum of 0.5 mM **C2** in MeCN.

Section SX: Spectral data for ligands and complexes.

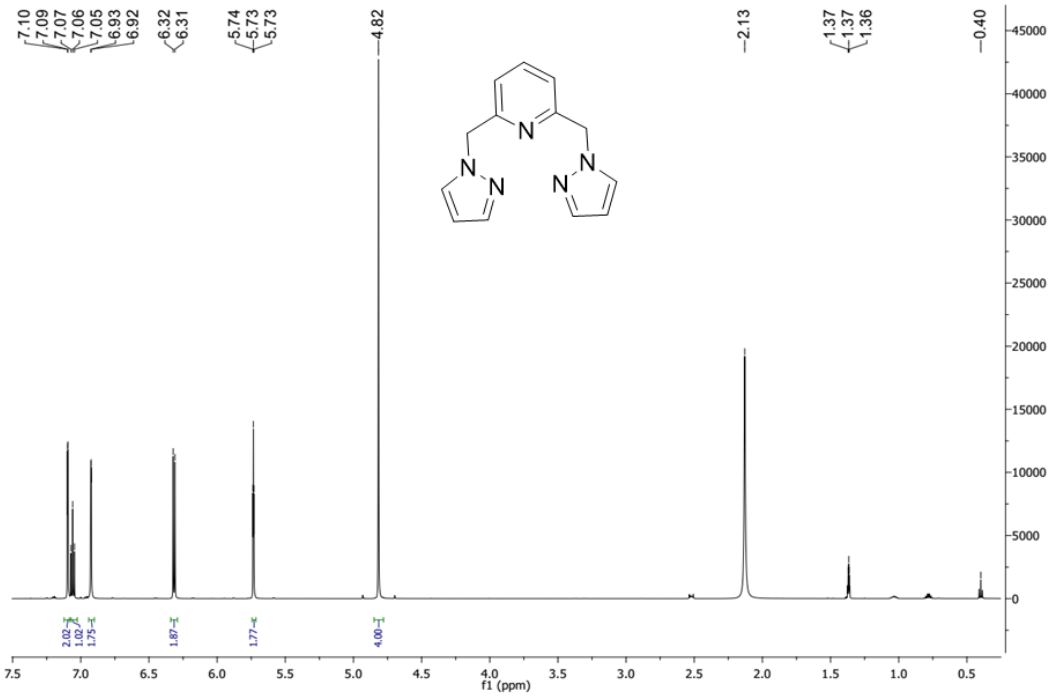

Figure S15: ^{1}H NMR spectrum for **L1**

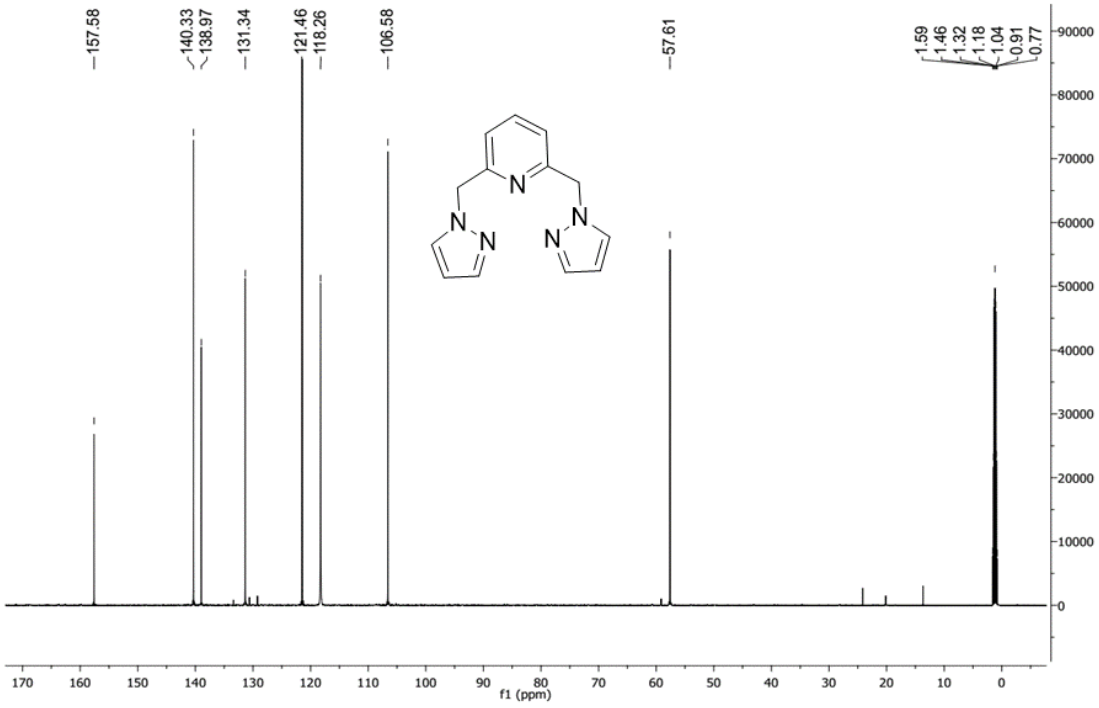

Figure S16: ^{13}C NMR for ligand **L1**

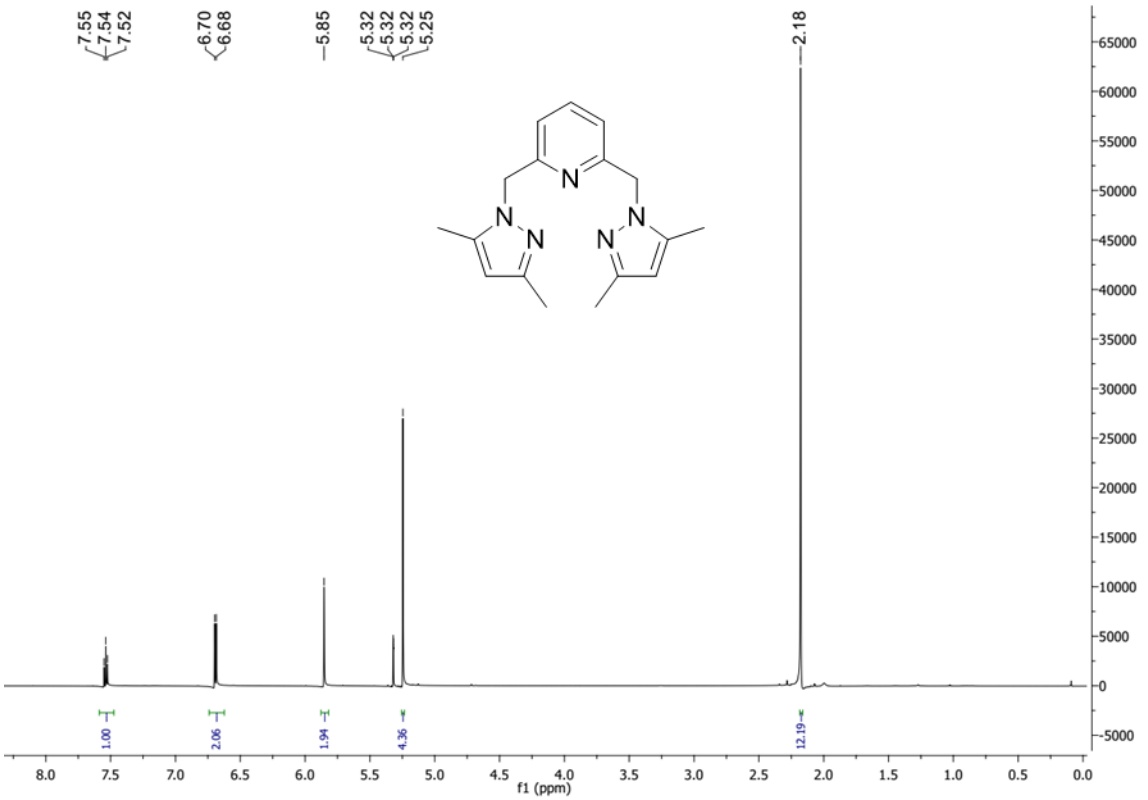

Figure S17: ^{1}H NMR spectrum for **L2**

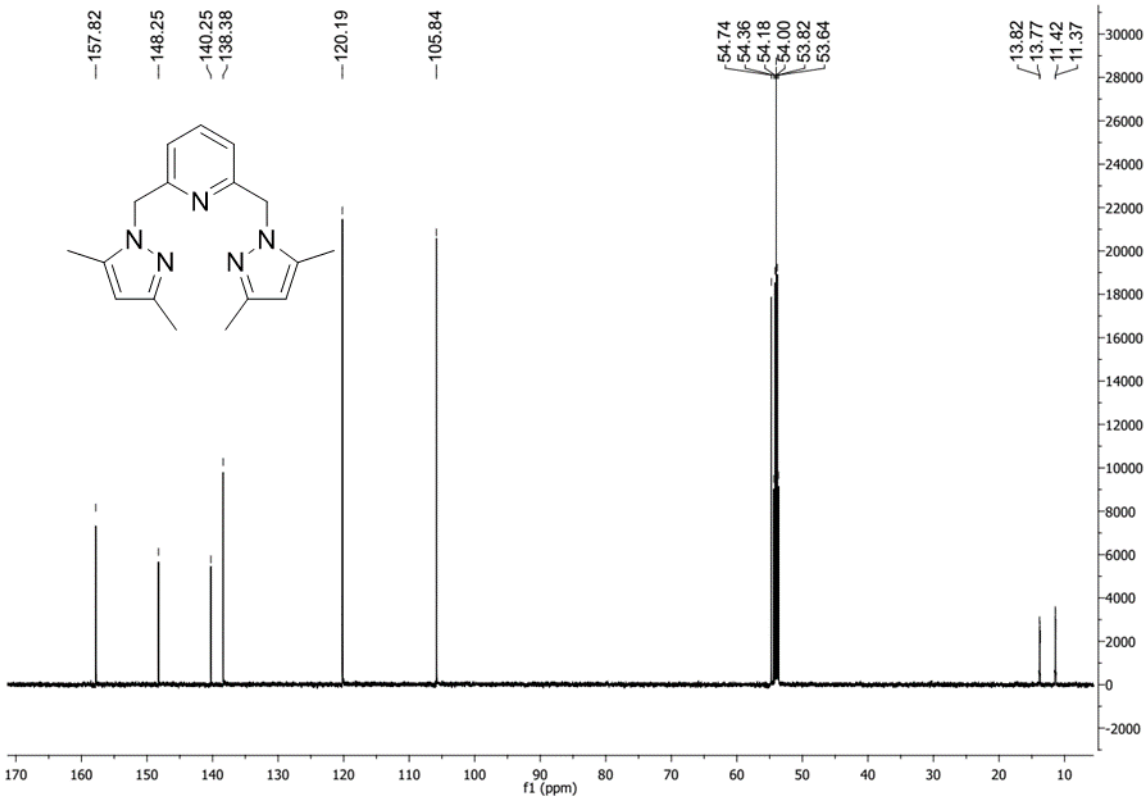

Figure S18: ^{13}C NMR spectrum for **L2**

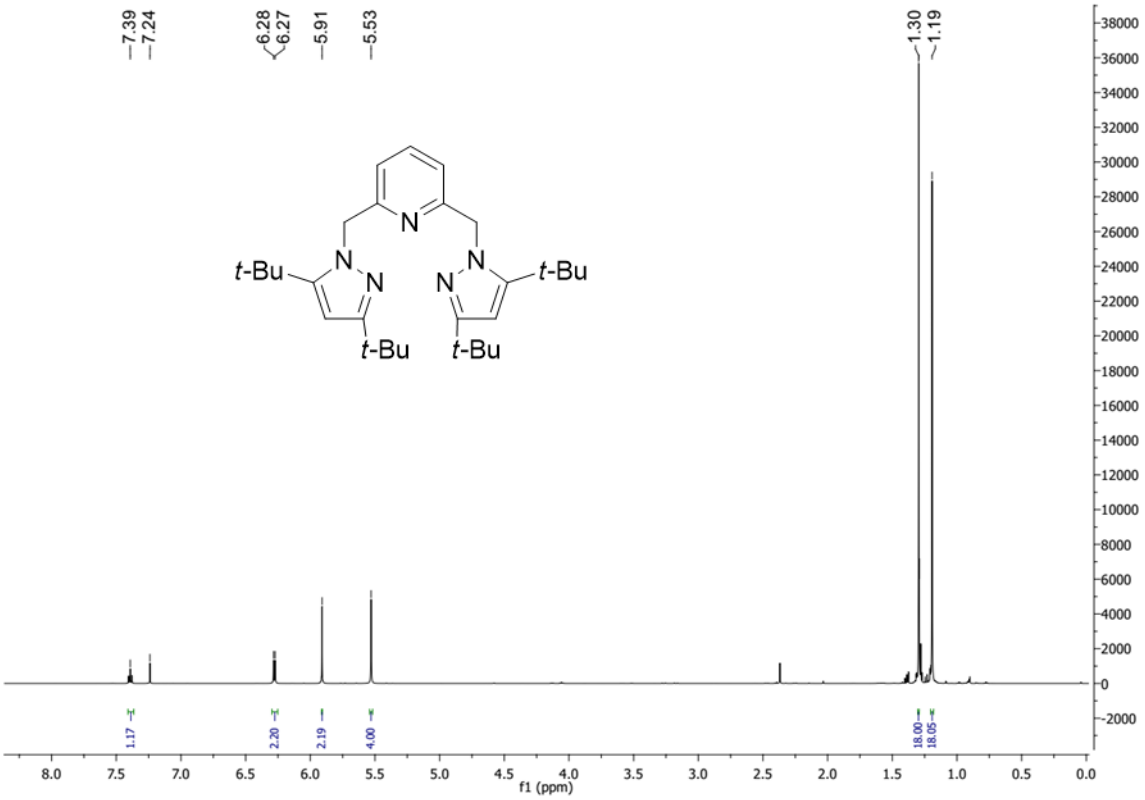

Figure S19: H NMR spectrum for **L3**

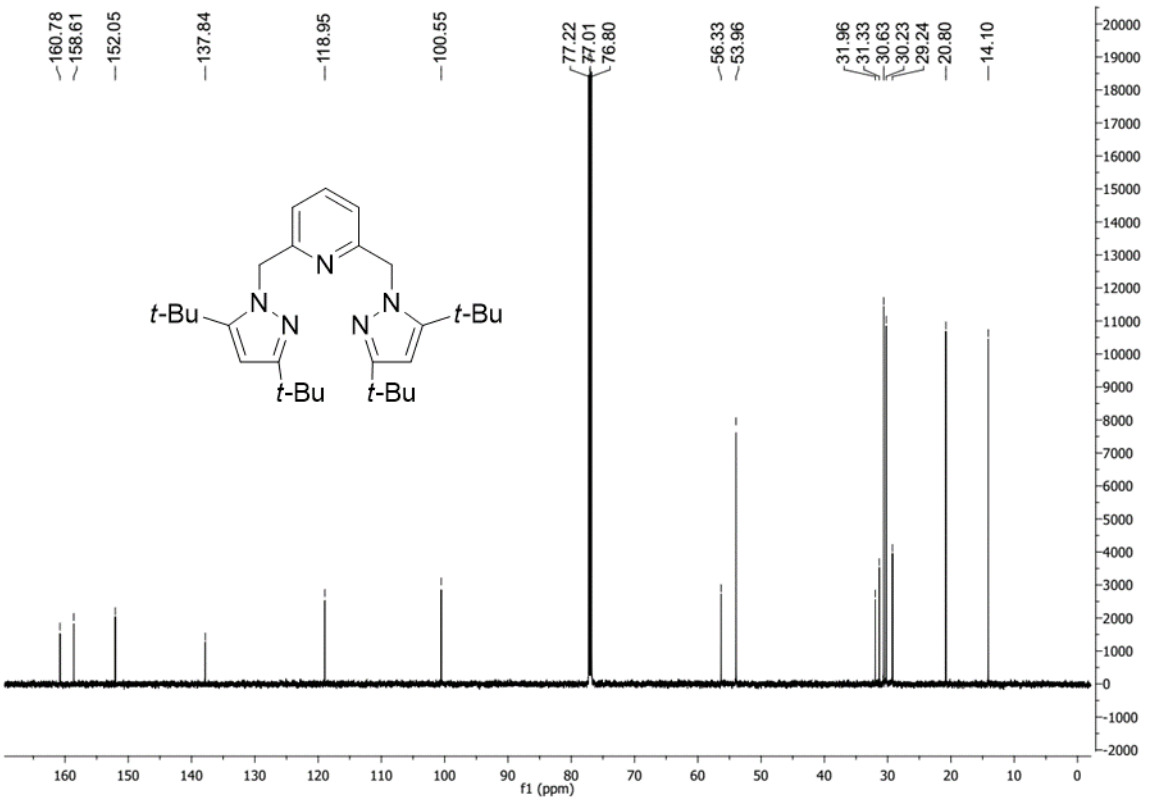

Figure S20: ^{13}C NMR spectrum for **L3**

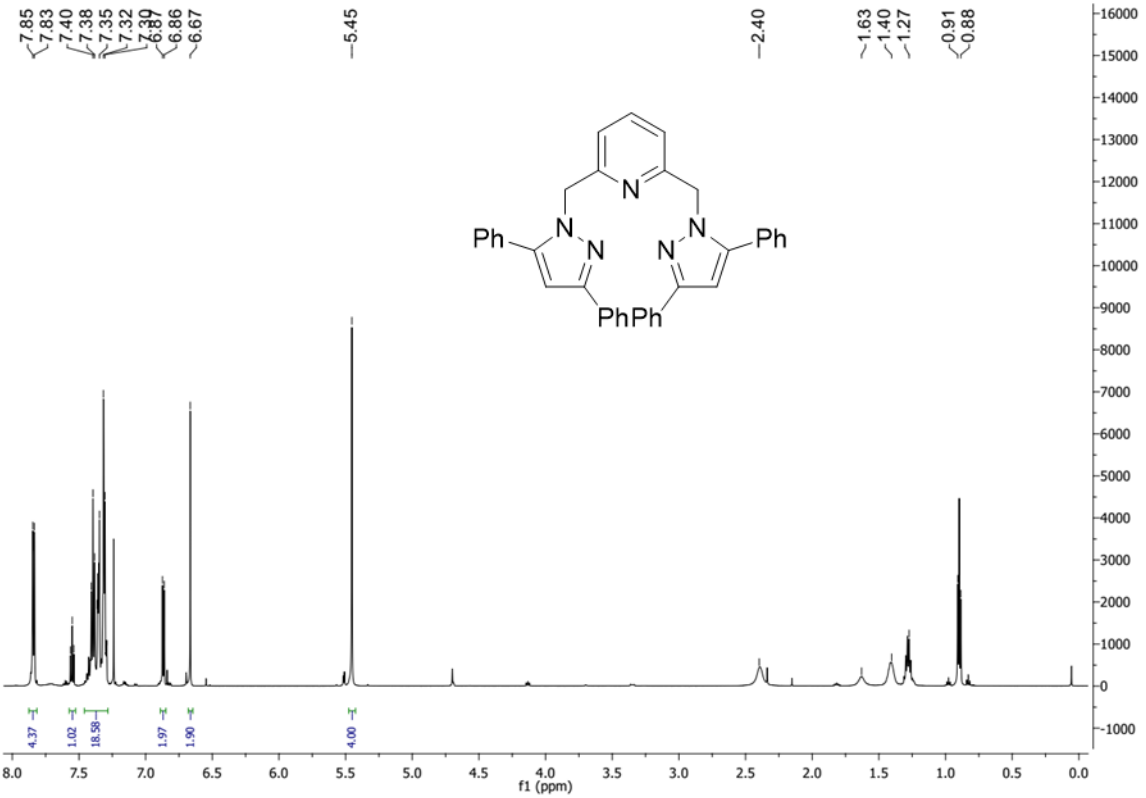

Figure S21: ^{1}H NMR spectrum for **L4**

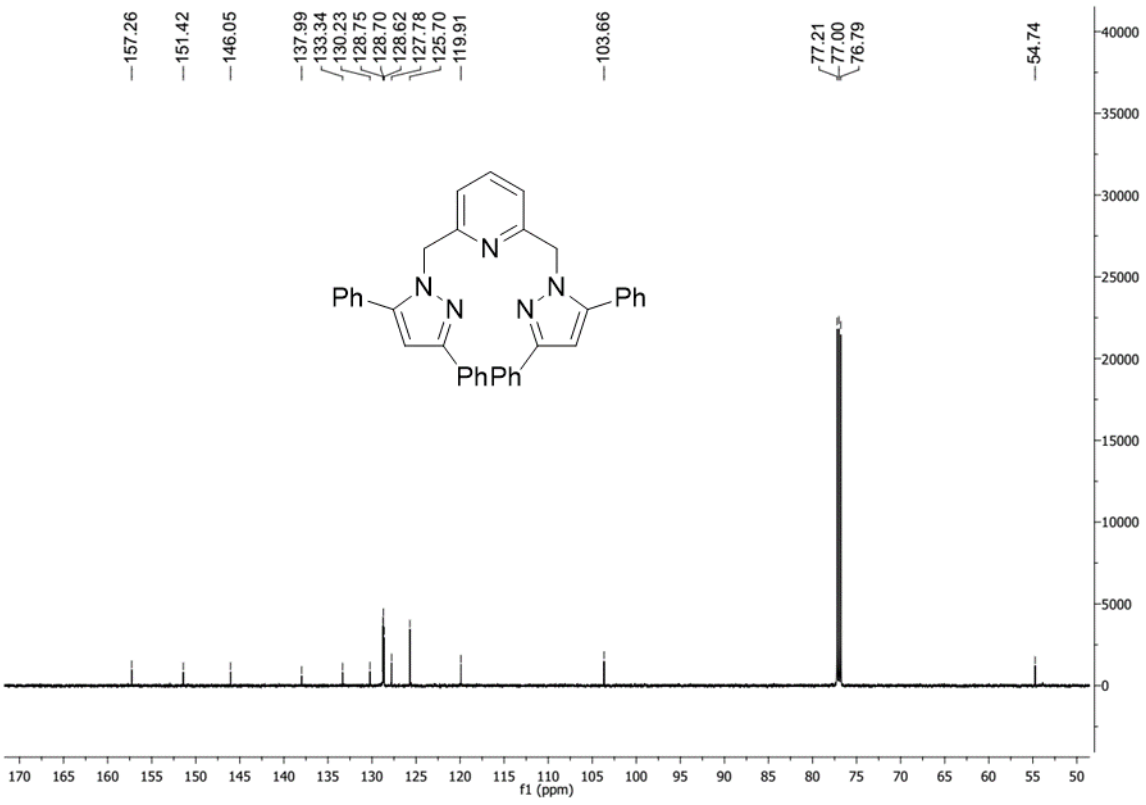

Figure S22: ^{13}C NMR spectrum for **L4**

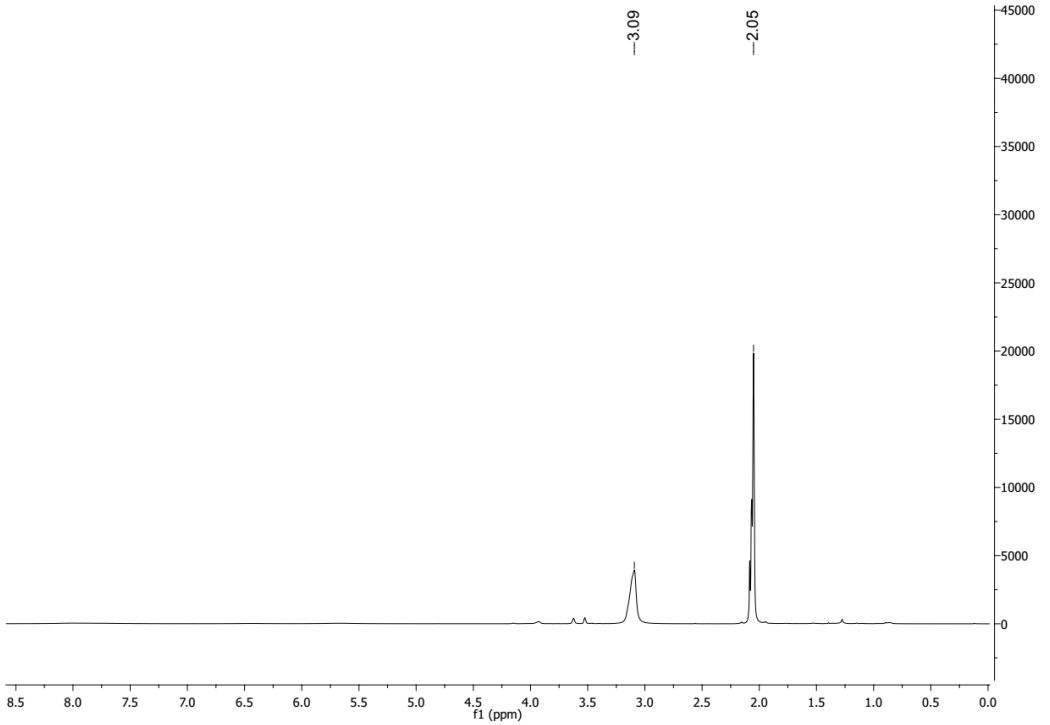

Figure S23: ^{1}H NMR spectrum of complex **C1** in Acetone-d_6

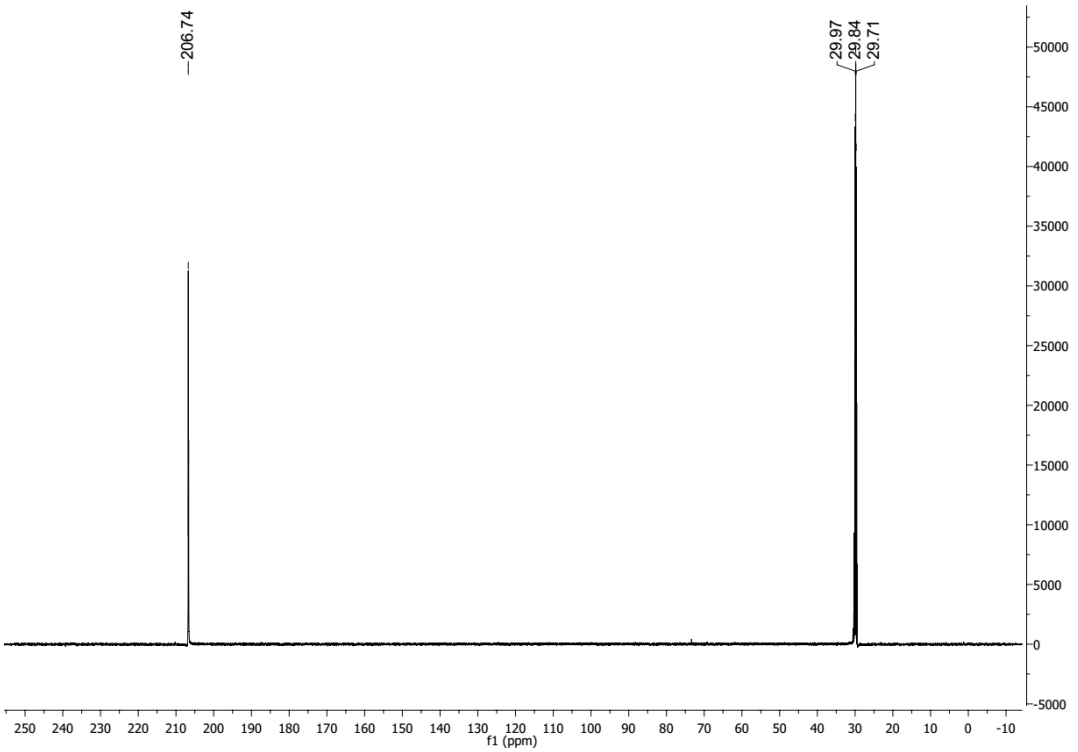

Figure S24: $^{13}C\{^{1}H\}$ NMR spectrum of complex **C1** in Acetone-d_6

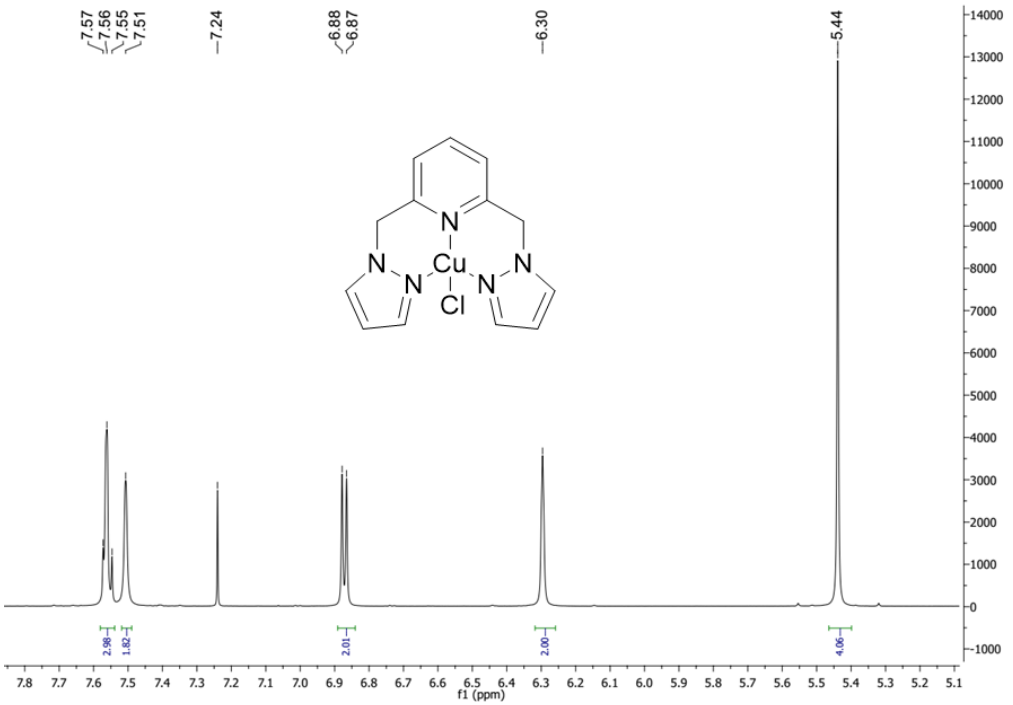

Figure 25: ^{1}H NMR spectrum of the chloro analogue of **C1** in $CDCl_3$

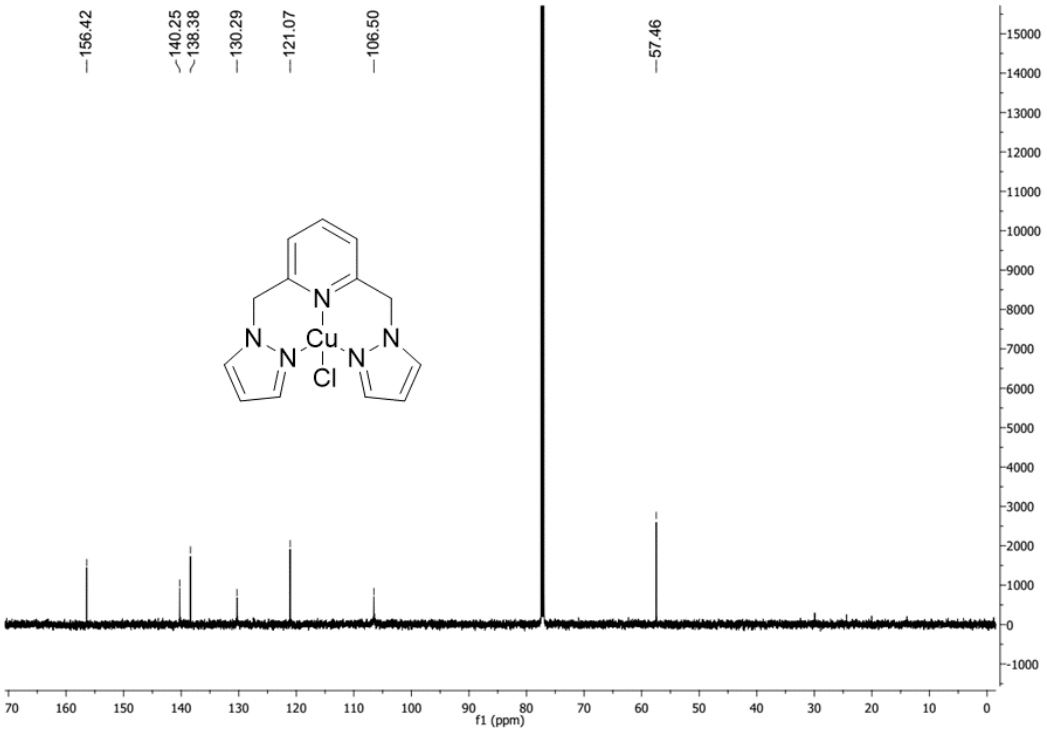

Figure S26: $^{13}C\{^{1}H\}$ NMR spectrum chloro analogue of **C1** in $CDCl_3$.

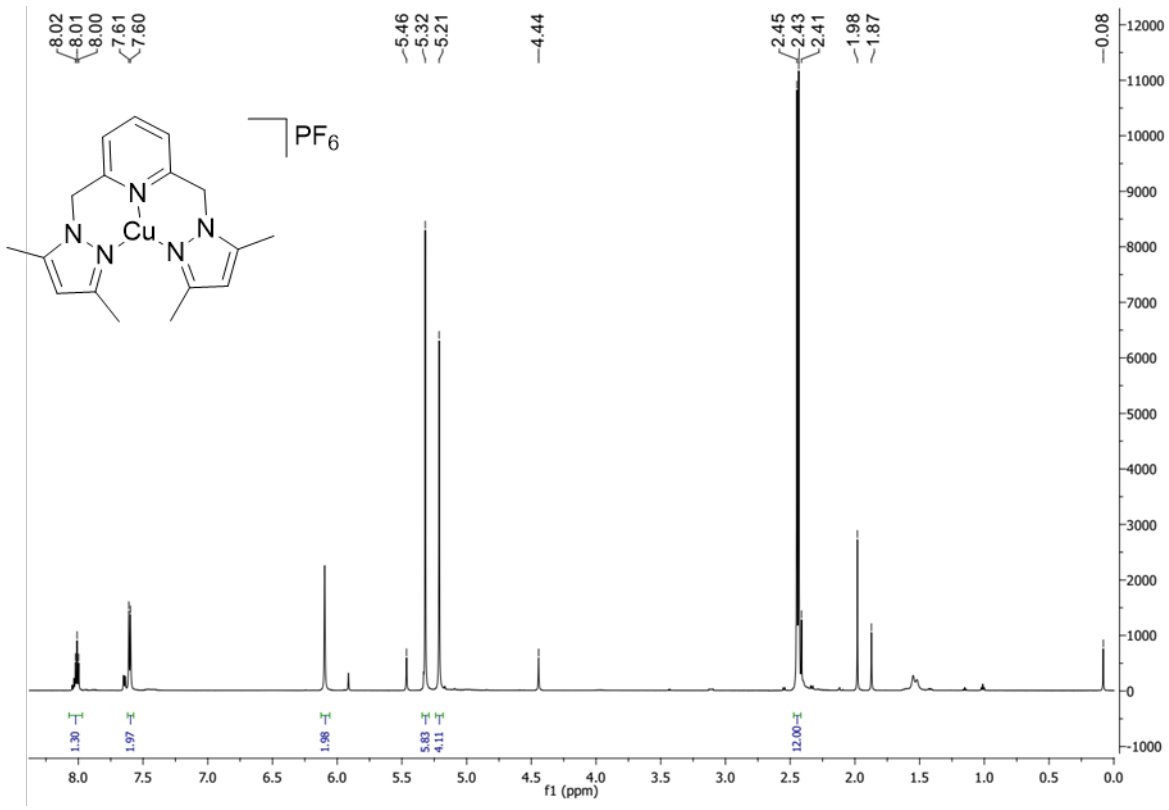

Figure S27: ^{1}H NMR spectrum for **C2**

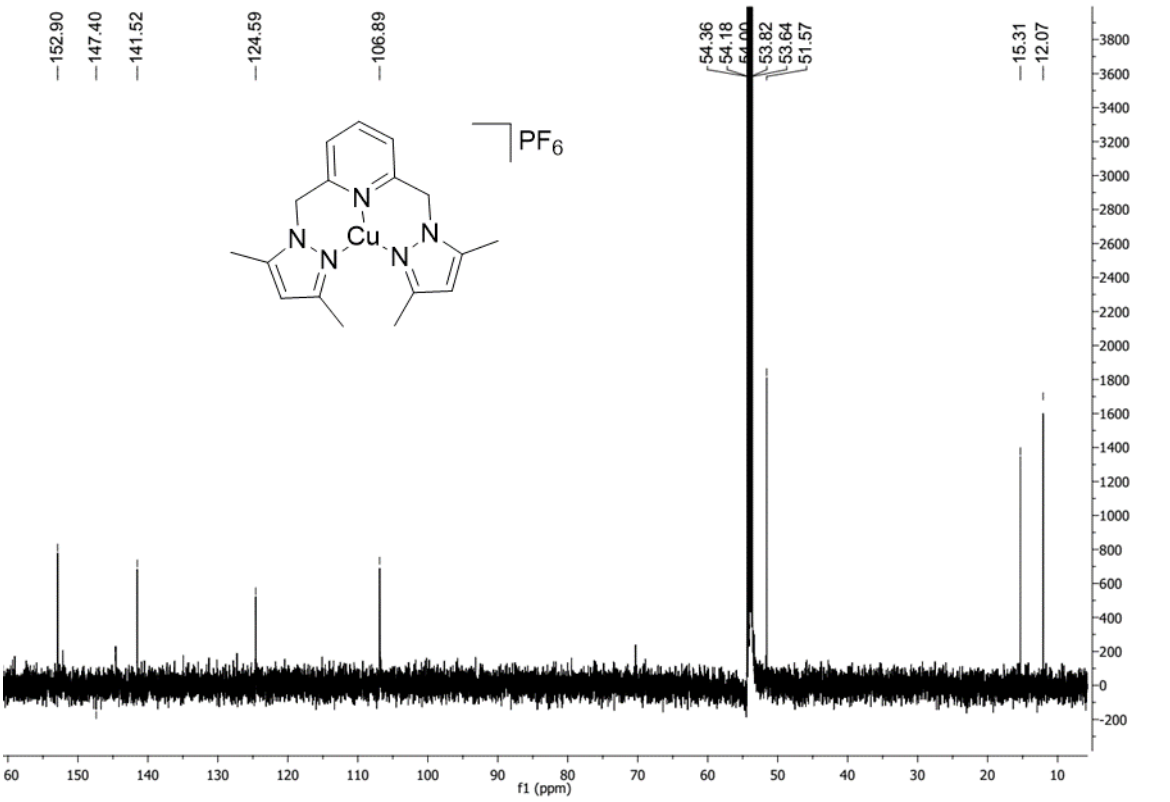

Figure S28: ^{13}C NMR spectrum for **C2**

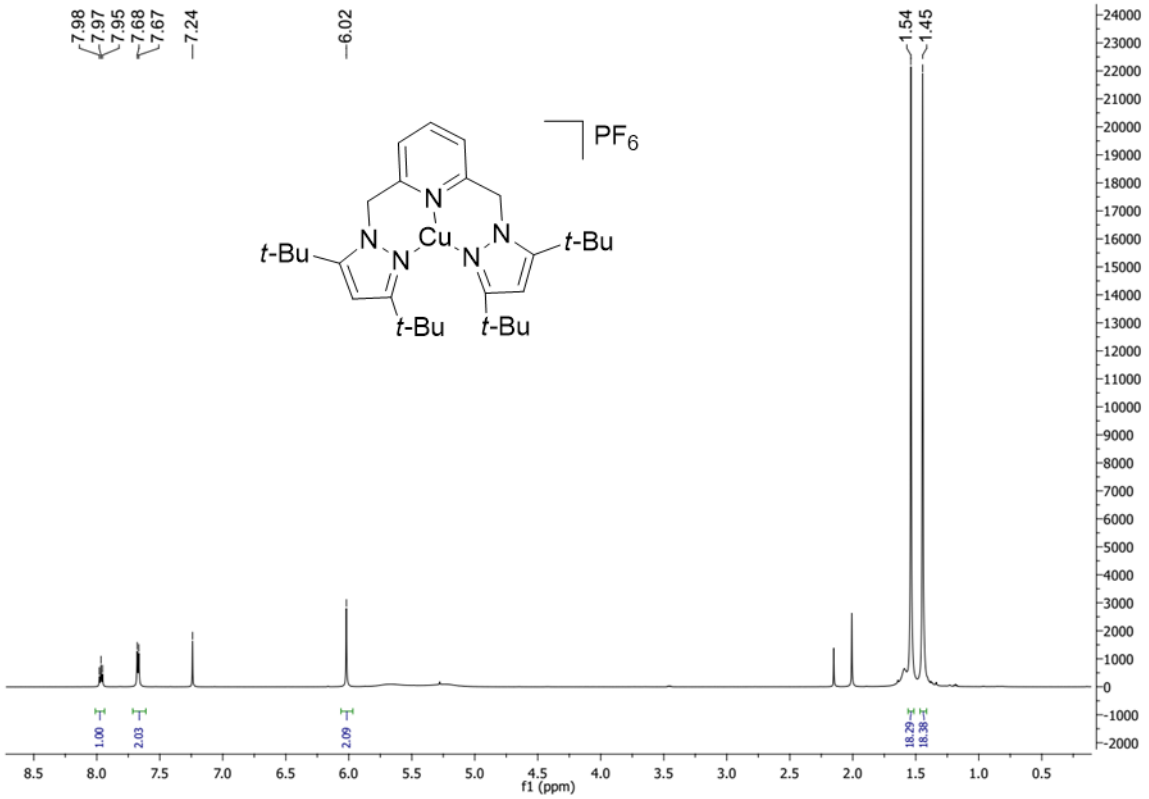

Figure S29: ^{1}H NMR spectrum for **C3**

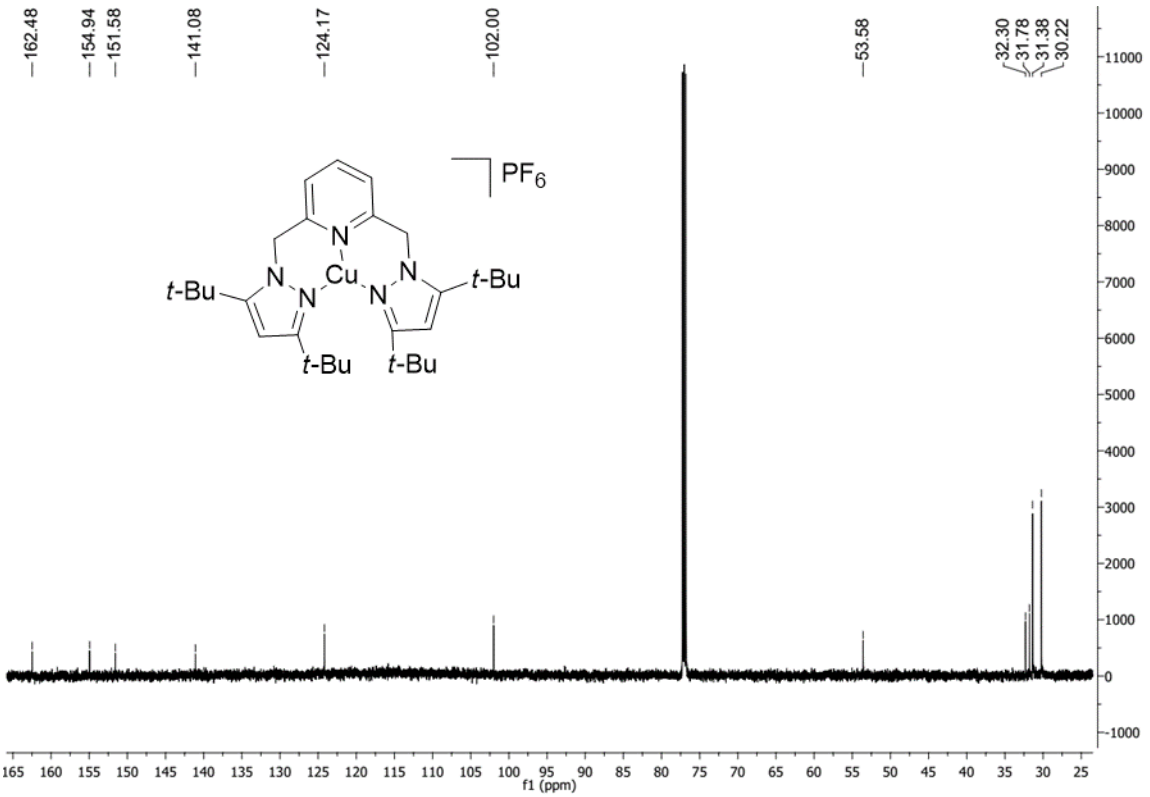

Figure S30: ^{13}C NMR spectrum for complex **C3**

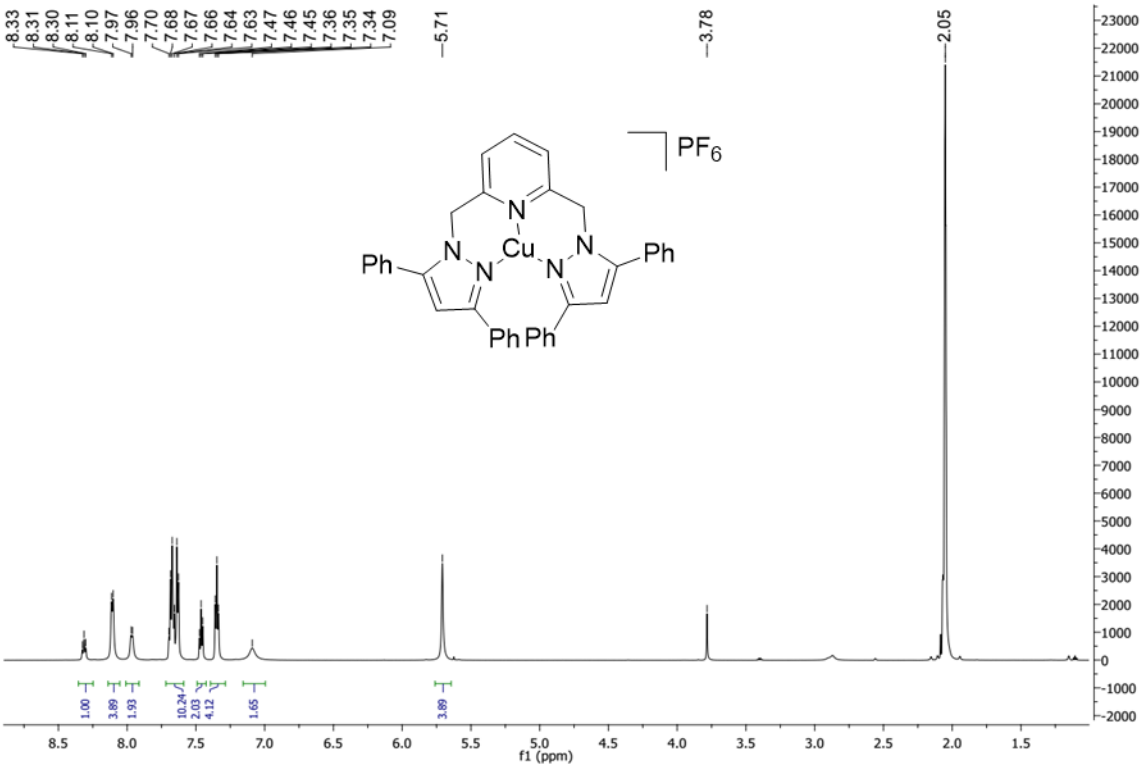

Figure S31: ^{1}H NMR spectrum for **C4**

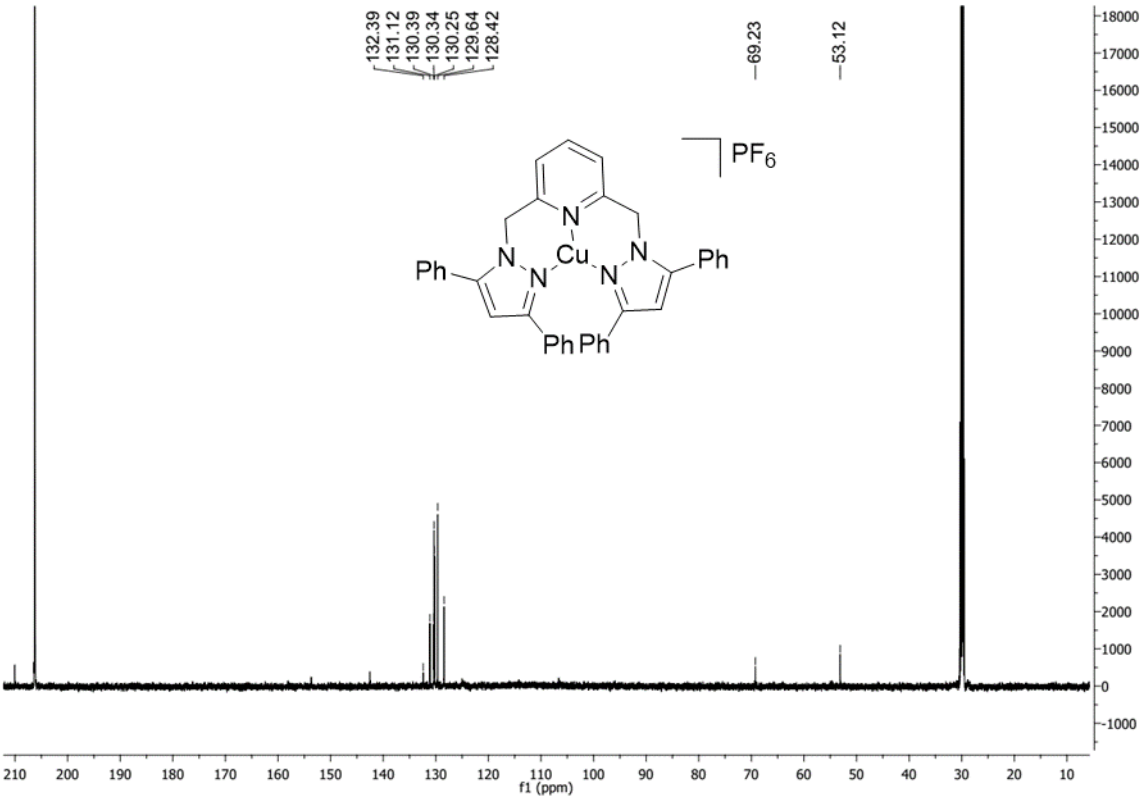

Figure S32: ^{13}C NMR spectrum for **C4**

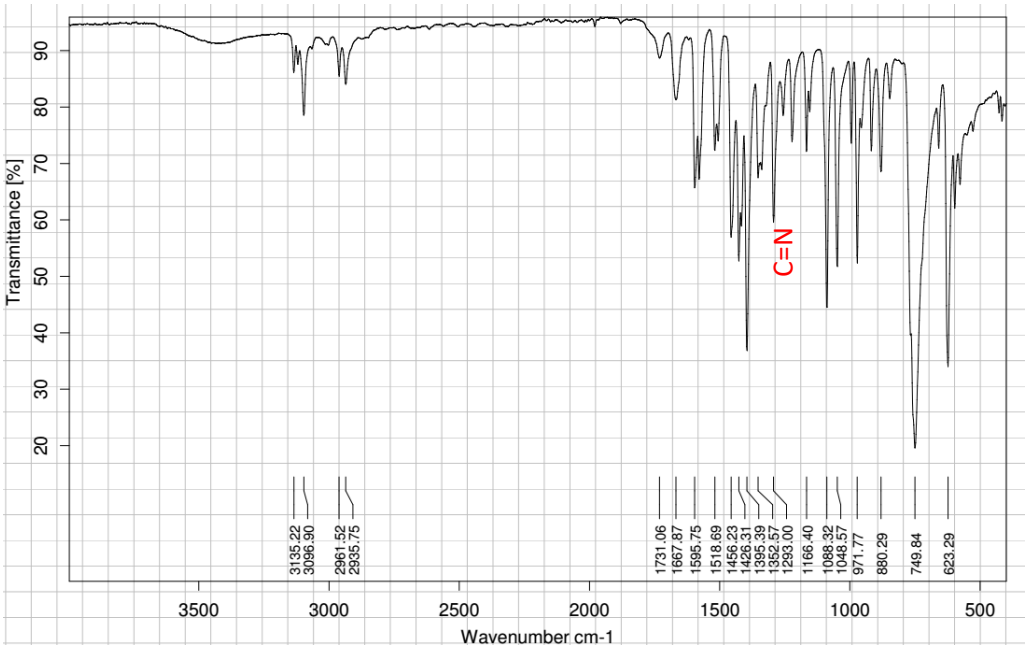

Figure S33: FTIR spectrum for **L1**

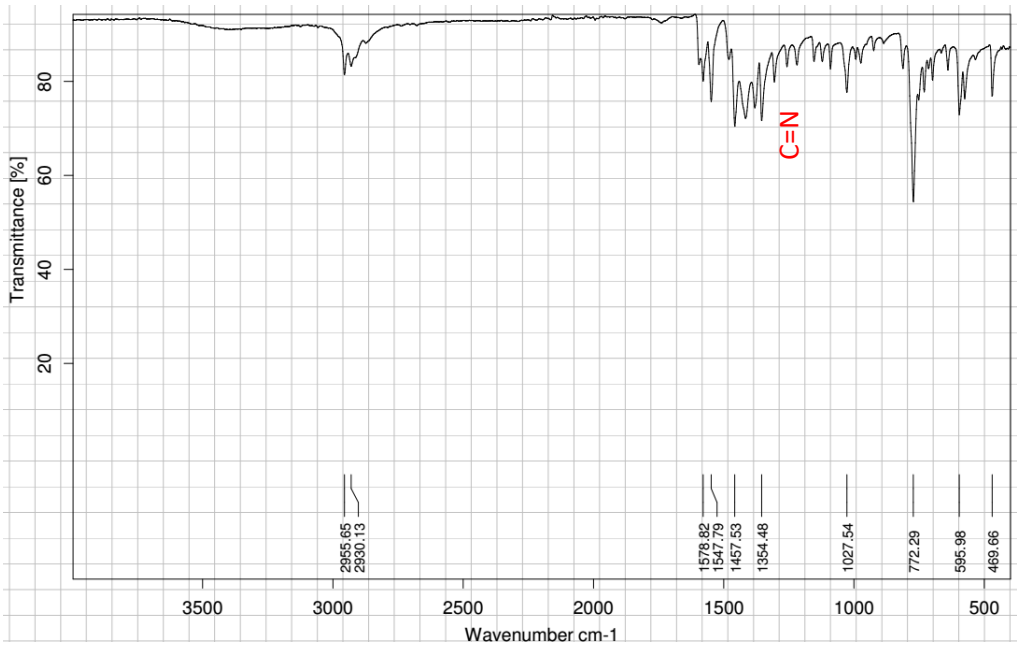

Figure S342: FTIR spectrum for **L2**

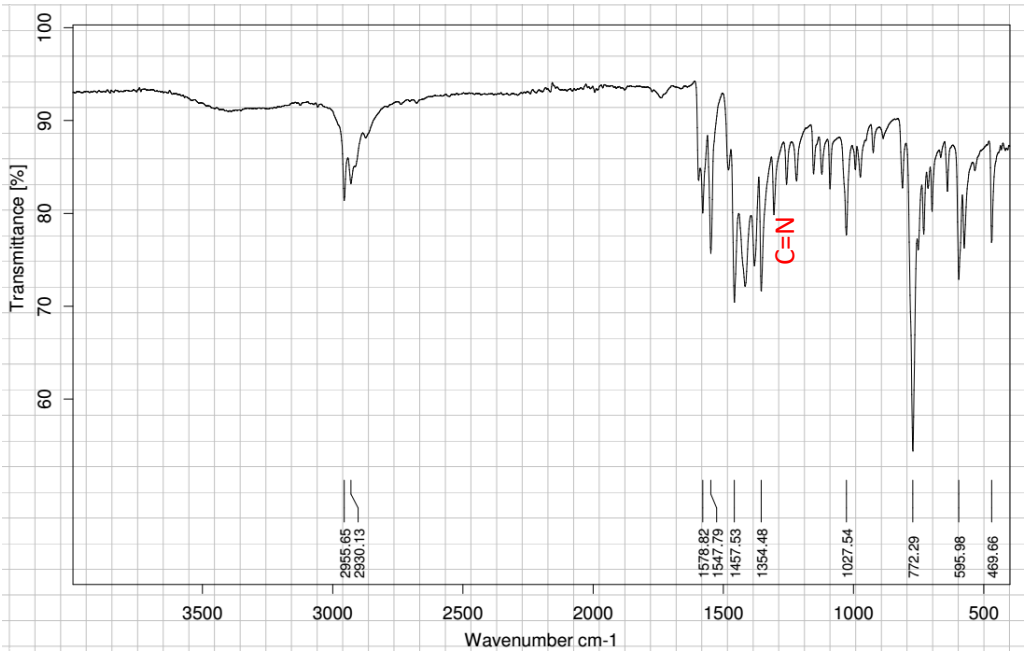

Figure S353: FTIR spectrum for **L3**

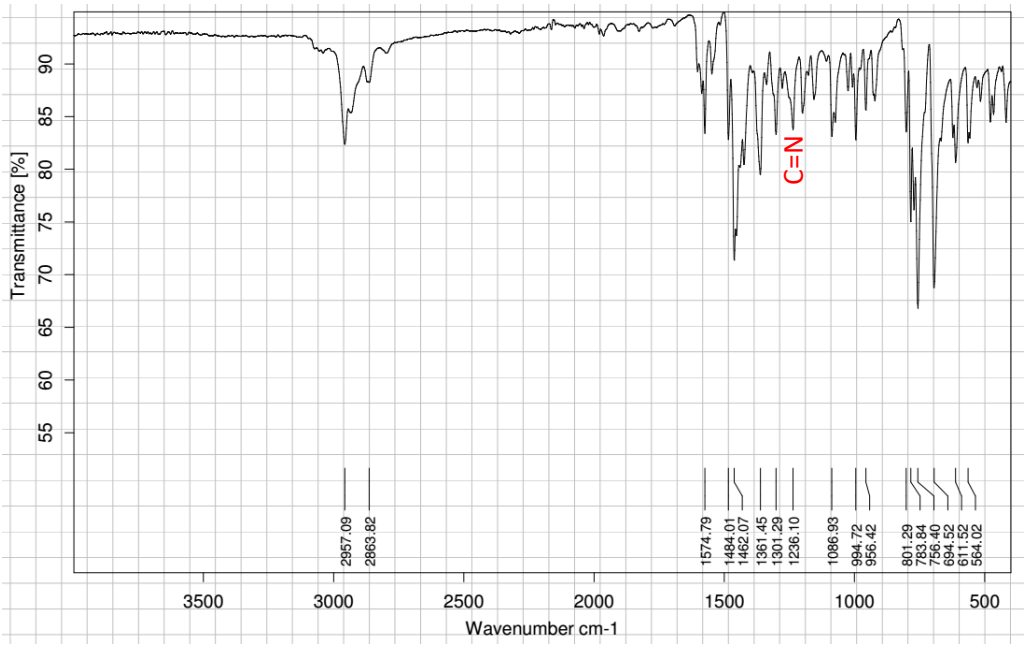

Figure S36: FTIR spectrum for **L4**

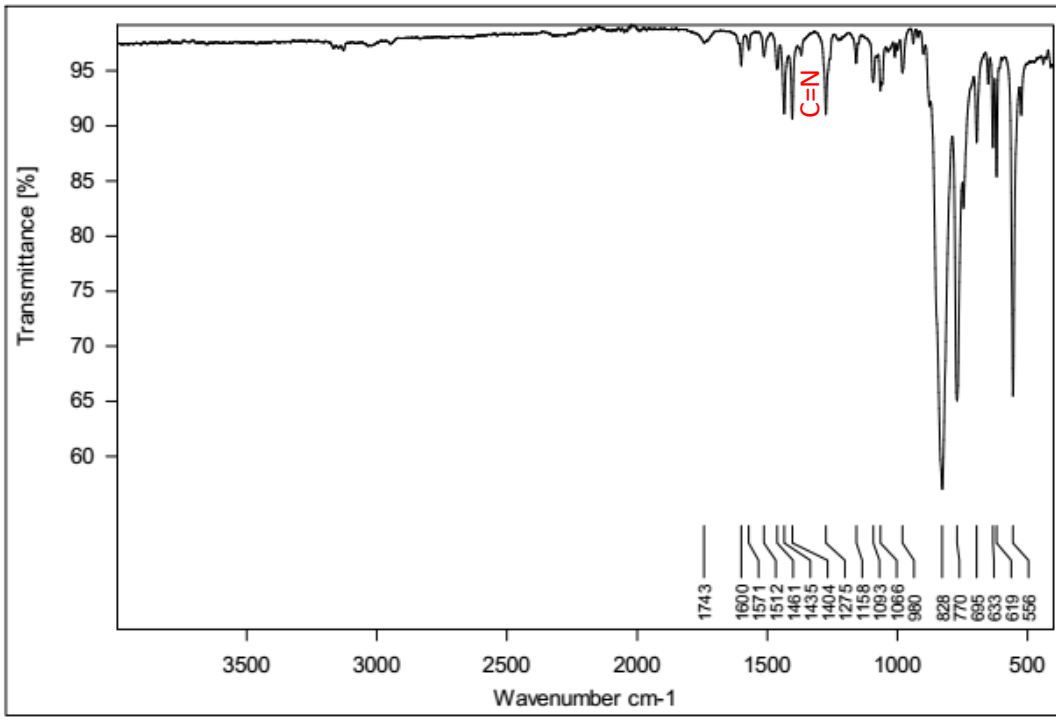

Figure S37: FTIR spectrum for **C1**

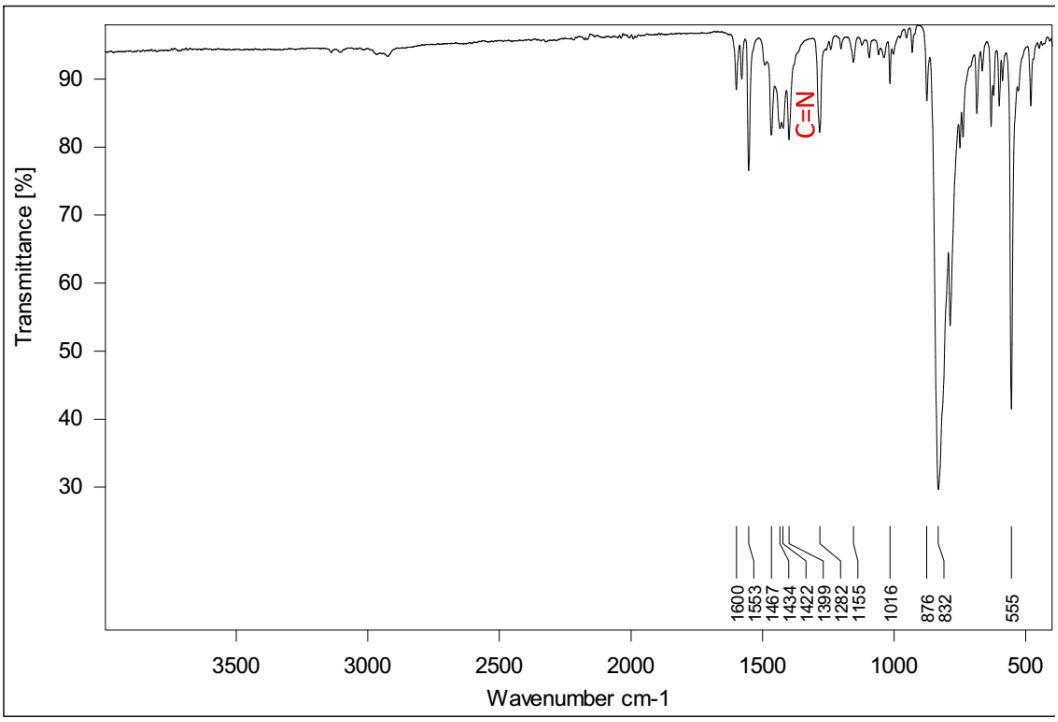

Figure S38: FTIR spectrum for **C2**

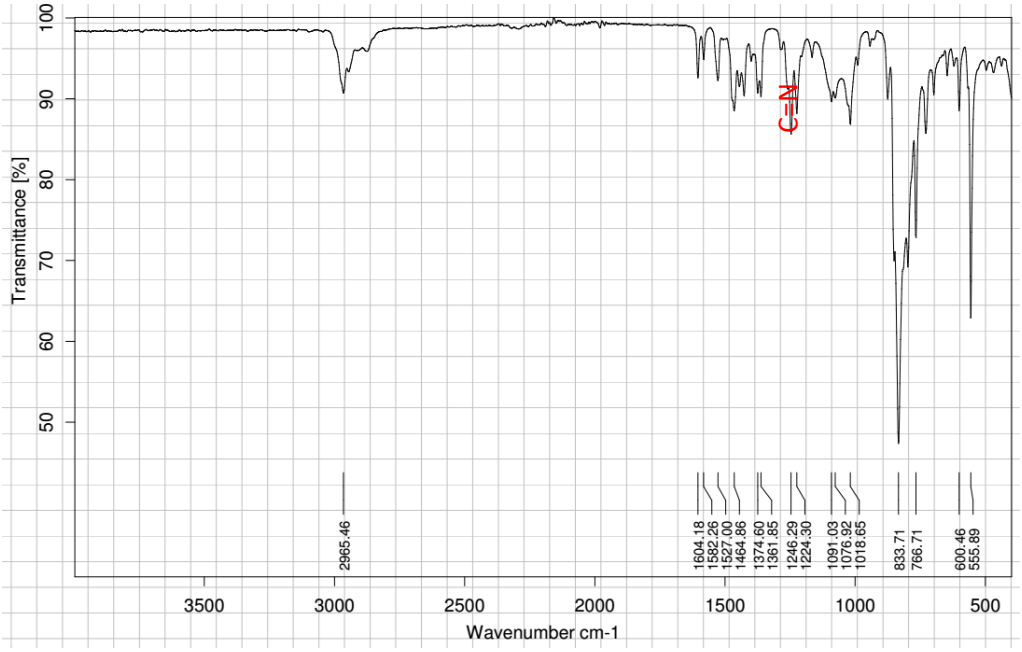

Figure S39: FTIR spectrum for **C3**

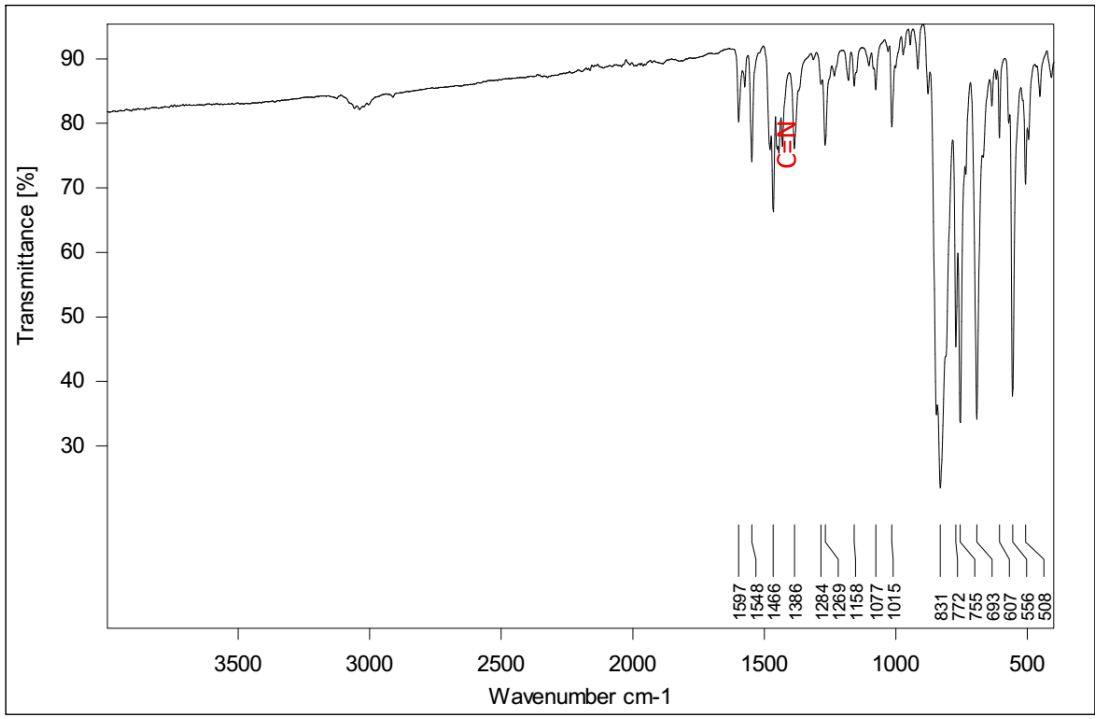

Figure S40: FTIR spectrum for **C4**

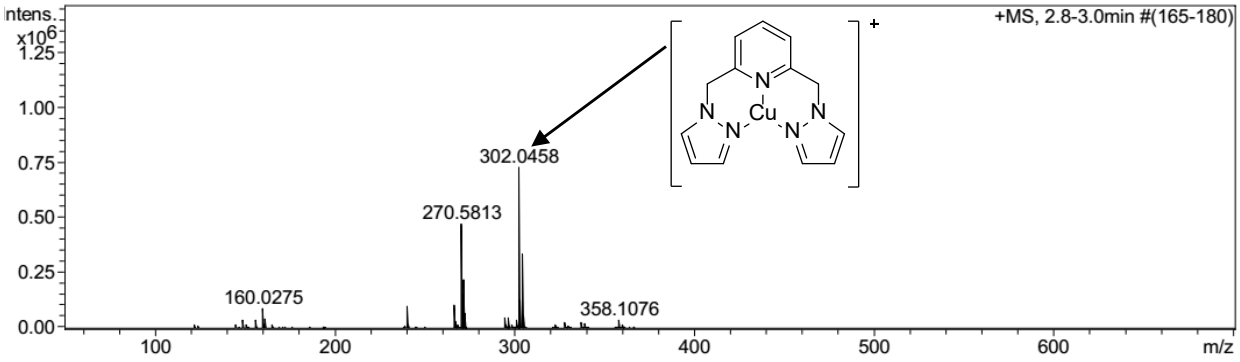

Figure S41: ESI-MS Spectrum for **C1**

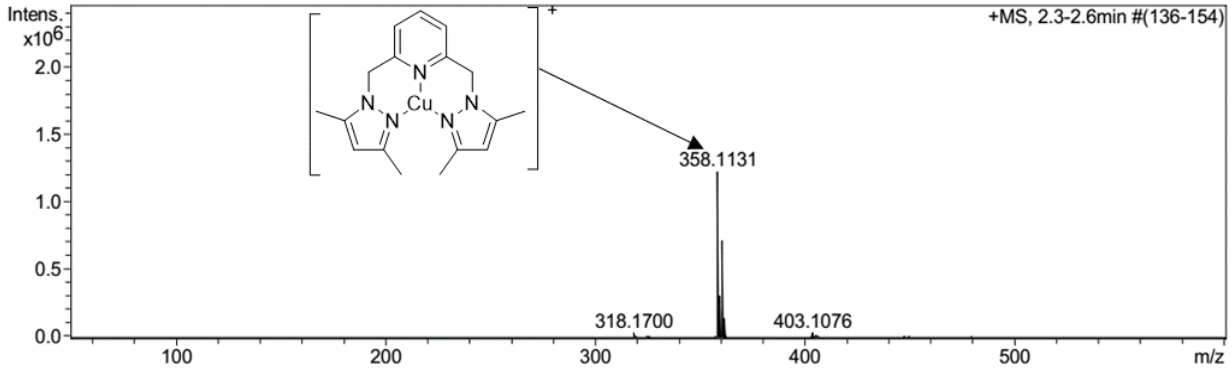

Figure S42: ESI-MS Spectrum for **C2**

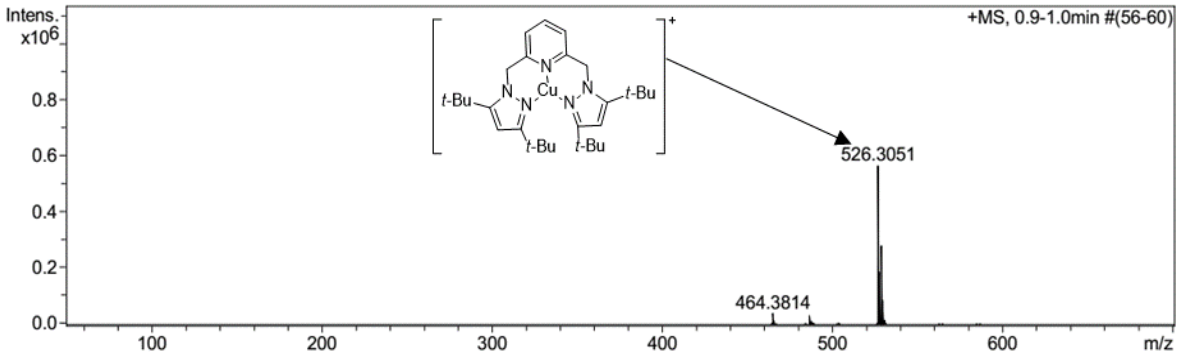

Figure S43: ESI-MS Spectrum for **C3**

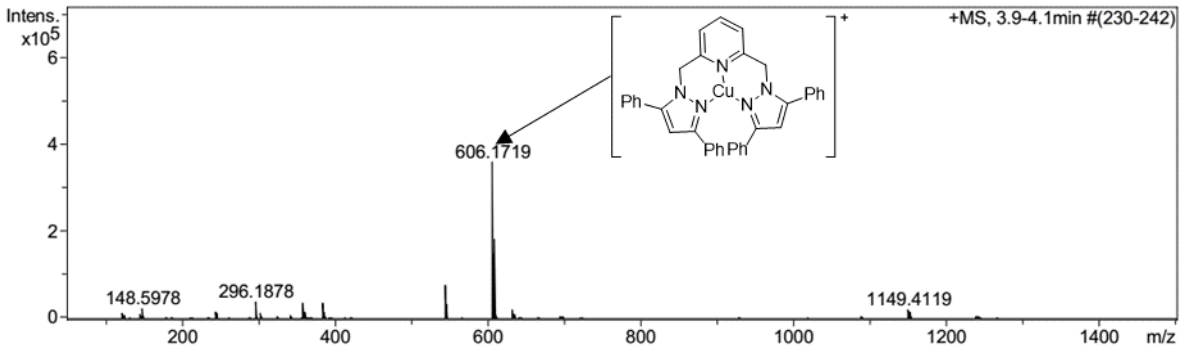

Figure S44: ESI-MS Spectrum for **C4**

References

1. J. L. V. Wyk, B. Omondi, D. Appavoo, I. A. Guzei and J. Darkwa, *Journal of Chemical Research*, 2012, 474-477.
2. (a) S. O. Ojwach, I. A. Guzei, L. L. Benade, S. F. Mapolie and J. Darkwa, *Organometallics*, 2009, **28**, 2127-2133; (b) A. A. Watson, D. A. House and P. J. Steel, *Inorganica Chimica Acta*, 1987, **130**, 167-176.
3. *SAINT*, *Version 8.38A*, Bruker AXS Inc, 2017.
4. *SADABS*, *Vesion 2012/1*, Bruker AXS Inc, 2012.
5. *APEX3*, *Version 2017.3*, Bruker AXS Inc, 2017.
6. G. Sheldrick, *Acta Crystallogr., Sect. C: Struct. Chem.*, 2015, **71**, 3-8.
7. (a) J. L. Atwood and L. J. Barbour, *Cryst. Growth Des.*, 2003, **3**, 3-8; (b) L. J. Barbour, *J. Supramol. Chem.*, 2001, **1**, 189-191.